ESTCP
Cost and Performance Report

(MM-9902)

Ultra-Wideband, Fully Polarimetric Ground Penetrating Radar for UXO Discrimination

May 2007

ENVIRONMENTAL SECURITY
TECHNOLOGY CERTIFICATION PROGRAM

U.S. Department of Defense

COST & PERFORMANCE REPORT
ESTCP Project: MM-9902

TABLE OF CONTENTS

Page

1.0 EXECUTIVE SUMMARY 1

2.0 TECHNOLOGY DESCRIPTION 5
- 2.1 OVERVIEW OF THE UWB, FULLY POLARIMETRIC GPR UXO CLASSIFICATION SYSTEM DEVELOPMENT AND ITS IMPLEMENTATION IN THE DEMONSTRATIONS 5
- 2.2 FULLY POLARIMETRIC UXO GPR 8
  - 2.2.1 RF Transceiver 8
  - 2.2.2 Antenna Unit 9

3.0 DEMONSTRATION DESIGN 11
- 3.1 PERFORMANCE OBJECTIVES 11
- 3.2 SURVEY, PROCESSING, AND INTERPRETATION METHODS 12
  - 3.2.1 Measurement Approach 12
  - 3.2.2 Preprocessing GPR Data 12
    - 3.2.2.1 Ensemble Background Subtraction 13
    - 3.2.2.2 Data Calibration 13
    - 3.2.2.3 Adaptive 2-D Spatial Smoothing 14
  - 3.2.3 Feature Extraction 14
- 3.3 UXO CLASSIFICATION RULES 15

4.0 CLASSIFICATION PERFORMANCE 17
- 4.1 BASELINE PERFORMANCE 17
- 4.2 PERFORMANCE IMPROVEMENT 19
- 4.3 ANALYSIS OF PERFORMANCE 22
- 4.4 PERFORMANCE COMPARISONS 24

5.0 COST ASSESSMENT 27
- 5.1 COST OF THE DEMONSTRATIONS 27
- 5.2 COST COMPARISONS AND POTENTIAL SAVINGS 28

6.0 IMPLEMENTATION, DISCUSSION, AND RECOMMENDATIONS 31

7.0 REFERENCES AND PUBLICATIONS 35

APPENDIX A POINTS OF CONTACT A-1
APPENDIX B THE GPR PROCESSING SYSTEM B-1

FIGURES

		Page
Figure 1.	Vector Network Analyzer (HP8712ET)	9
Figure 2.	Diagram of the Bottom View and Side View of the OSU-ESL UWB Full-Polarization GPR Antenna.	10
Figure 3.	UXO GPR Configuration Used at Blossom Point, JPG, and Fort Ord Sites, with Antenna Arms Aligned with and Perpendicular to the Travel Direction.	10
Figure 4.	Classification ROC Curves Based on TRUE UXO Criterion and on UXO-LIKE Criterion with Dashed Line of No Discrimination.	18
Figure 5.	ROC Curves for Fort Ord Showing Performance Obtained from GPR Alone and Improvement from Inclusion of Mag Dipole Presence as a Factor (left) and ROC Points from Different Rounds of Processing at JPG-V using TRUE-UXO, LD >2, and LD >3 Criteria (right).	20
Figure 6.	Based on JPG-V and Fort Ord-GPR Data Alone, for Correctly Classified UXO-Like Items: Absolute Depth Estimation Error (left) and Absolute Length Estimation Error (right)	21
Figure 7.	ROC Curves for the Tyndall Site for Various Ordnance Types, Obtained When ETL Was Included in the Criteria for 105 mm Projectiles of Different Length Error Tolerance (left) and for Various Ordnance Types with Sufficient Length Tolerance to Reach 100% Pd (right)	22
Figure 8.	MTADS Discrimination Using Mag Data Alone (red); Enhanced Results Obtainable from MTADS Mag Data, Including Mag Dipole Orientation Information (green); and Results Including Information from "three β" EMI Data (blue) (ESTCP).	25

TABLES

		Page
Table 1.	Rule for Class Upgrade When Magnetic Dipole Is Present	19
Table 2.	Labor and Activity Costs of the Demonstrations	27
Table 3.	Equipment Costs of the Demonstrations	28

ACRONYMS AND ABBREVIATIONS

AERTA	Army Environmental Requirements and Technology Assessment
AFB	Air Force Base
BP	Blossom Point
CNR	complex natural resonance
CRREL	Cold Regions Research and Engineering Laboratory
DEN	density
DoD	Department of Defense
ELF	estimated linearity factor
EMI	electromagnetic interference
ERDC	Engineer Research and Development Center
ESTCP	Environmental Security Technology Certification Program
ETL	estimated target length
ETO	estimated target orientation
GPR	ground-penetrating radar
GPS	global positioning system
HFB	horn-fed bowtie
IFFT	inverse fast Fourier transform
JPG	Jefferson Proving Ground
L/D	length-to-diameter
LOND	line of no discrimination
Mag	magnetometry
MTADS	Multi-Sensor Towed Array Detection System
NRL	Naval Research Laboratory
OSU-ESL	Ohio State University Electroscience Laboratory
Pd	probability of detection
Pfa	probability of false alarm
PI	principal investigator
RF	radio frequency
ROC	receiver operating characteristics

SCR	signal-to-clutter ratio
SERDP	Strategic Environmental Research and Development Program
SNR	signal-to-noise ratio
TEM	transverse electromagnetic
USACE	U.S. Army Corps of Engineers
UWB	ultra-wideband
UXO	unexploded ordnance
VNA	vector network analyzer

ACKNOWLEDGEMENTS

With the support of the Environmental Security Technology Certification Program (ESTCP) under Project 199902 and Dr. Jeffrey Marqusee, Director, the ground-penetrating radar (GPR) work reported herein was carried out by a joint team of personnel from the Ohio State University Electroscience Laboratory (OSU-ESL), the U.S. Army Corps of Engineers (USACE), Engineer Research and Development Center (ERDC), Hanover site Cold Regions Research and Engineering Laboratory (CRREL). The principal investigator (PI) was Dr. Kevin O'Neill of ERDC, with the OSU-ESL's Dr. Chi-Chih Chen as Co-PI. Dr. Chen was at the heart of the project at all times, performing the most essential tasks and giving crucial guidance in all aspects of the work. Dr. Richard Detsch of ERDC-CRREL assisted in planning and executing initial fieldwork. Dr. Chen's graduate students, Matthew B. Higgins and Hyoung-Sun Youn, were invaluable and extraordinarily assiduous in everything from design and construction of equipment to mathematical modeling, execution of fieldwork, and processing and interpretation. All of us benefited from the deep wisdom as well as the occasional direct guidance of Professor Leon Peters, Jr., now retired from the OSU-ESL and widely acknowledged as one of the pioneers of GPR.

Computational and modeling work supporting the data processing and interpretation was provided by Professor Robert Lee of the OSU Department of Electrical Engineering and by his students, including Kishore Rama Rao and Kwan-Ho Lee. Dr. Fridon Shubitidze of the Thayer School of Engineering at Dartmouth also performed modeling work and participated in the execution of some fieldwork.

This diverse, talented, and dedicated team merits heartfelt thanks for contributing in such an exemplary manner to the successful execution of the project.

Technical material contained in this report has been approved for public release.

This page left blank intentionally.

1.0 EXECUTIVE SUMMARY

This project addressed the Tri-Service Environmental Quality Research, Development, Test, and Evaluation Strategic Plan, unexploded ordnance (UXO) requirements, which state in part [1].

> *There are more than twenty million acres of bombing and target ranges under DoD control.... Each year a significant fraction (200,000-500,000 acres) of these spaces are returned to civilian (Private or Commercial) use. All these areas must be surveyed for buried ordnance and other hazardous materials, rendered certified and safe for the intended end use. This is an extremely labor intensive and expensive process, with costs often far exceeding the value of the land.… Improved technologies for locating, identifying and marking ordnance items must be developed to address all types of terrain, such as open fields, wooded areas, rugged inaccessible areas, and underwater sites.*

Similar requirements are reflected in the U.S. Army Requirement A(1.6a), titled: Unexploded Ordnance (UXO) Screening, Detection, and Discrimination [2] and described in the FY99 Army Environmental Requirements and Technology Assessments (AERTA). This Army requirement has been ranked as the highest priority user need in the Environmental Cleanup Pillar. In addition, this project addressed the UXO detection and discrimination requirements and recommendations described in the Defense Science Board Task Force Final Report on UXO Clearance and Remediation published in 1998 [3]. In response to these regulatory requirements, demonstrations were carried out for the purpose of establishing the buried UXO discrimination capabilities of an ultra-wideband (UWB), fully polarimetric GPR. The GPR system and processing were intended to incorporate the broadest capabilities and most current sophistications available so that some speculations could be made as to the discrimination capabilities of current GPR technology per se, not simply of the system used in the tests. That said, it would not be surprising if other practitioners and systems showed somewhat different results, especially as the technology and techniques of application advance so rapidly. As regards the system reported on here, a new generation has already proceeded beyond the characteristics described below.

Here "discrimination" means cued surveying, sorting unseen objects into UXO and non-UXO classes, given previously identified locales where some kind of signal anomalies have been recorded. This contrasts with "straight detection," meaning simply identification and location of the signal anomalies. The emphasis in straight detection is on finding as many UXOs as possible, with only secondary consideration of false alarm rate. The emphasis in discrimination, as the word is used here, is on correct classification, maximizing correct "dig" decisions while minimizing false alarms.

The demonstrations in this project took place between January 2000 and November 2001 at four sites: Tyndall Air Force Base (AFB); Blossom Point, Maryland; Jefferson Proving Ground (JPG), Madison, Indiana; and the former Fort Ord in Monterey, California. Time requirements at each site is listed in Section 5. The one-of-a-kind GPR could operate from about 10 MHz to 810 MHz and was fully polarimetric. The implication of full polarimetry is that complete amplitude and phase information is obtained for orthogonal and cross channels. Given these measurements

for any particular antenna rotation (polarization), the copolarization and cross-polarization responses can be synthesized for any other polarizations of transmission and reception. These features allowed operators and analysts to identify basic discrimination parameters, including prominently the estimated target depth, horizontal plane location, orientation, complex (frequency) natural resonance, length, linearity factor, and density of signal about the most prominent polarization orientation, as well as spatial distribution of some of those parameters along survey scans. Estimated linearity factor (ELF), in connection with various of the others, is probably the most crucial of these for the classification processing sequence that was applied. That processing was designed to ascertain whether or not the received signal should be construed as coming from an object with the overall geometry of a UXO. Correct sorting of unknown targets into the UXO class counts here as a "detection," while incorrect sorting into that class counts here as a "false alarm." In keeping with these definitions, processed results are presented in terms of probability of detection (Pd) and probability of false alarm (Pfa):

$$Pd \equiv \frac{Number\ of\ correct\ UXO\ classifications}{Total\ number\ in\ UXO\ class}$$

$$Pfa \equiv \frac{Number\ of\ incorrect\ UXO\ classifications}{Total\ number\ in\ UXO\ class}$$

Performance was quantified and analyzed in terms of receiver operating characteristics (ROC) curves, which show Pd on the vertical axis versus corresponding Pfa on the horizontal axis, as decision criteria are loosened or tightened. In these terms, a system shows discrimination capability better than would be obtained from completely arbitrary or random guesses when the ROC curve lies above the 45E line between (0,0) and (100%, 100%) in the Pfa-Pd plane, called here the "line of no discrimination" (LOND). Relative to the LOND, the GPR system that was demonstrated exhibited definite discrimination capability in its baseline performance. Also, despite considerable variation of relevant environmental, e.g., soil factors, the ultimate ROC performance pattern was similar for the different ultimate sites. Before various improvements were applied, about a 55% Pd of UXO-like targets was obtained with only a 10% Pfa; however, progress along the curve to 90% Pd was achieved only slowly after reaching about 80% Pfa. Thus, the primary limitation of the system could be viewed as difficulty achieving high or 100% Pd. Another performance standard is obtained if, instead of sorting items in the target set in terms of whether or not they are UXO-like in geometry, one sorts them instead according to TRUE UXO identity, regardless of object geometry ("TRUE UXO" criterion). In this case the ROC curve performance is distinctly worse. Under this TRUE UXO criterion the system shows definite discrimination capability but not very much. It is greater than unity over the entire Pfa range, with a peak Pd/Pfa ratio at 50/30%. The UXO-like criterion was pushed here because this is what in fact most classification schemes pursued by others ultimately employ, and because site managers presumably will dig up anything that their processing system indicates is geometrically UXO-like, even if positive identification as a UXO cannot be provided.

Various processing improvements were tested, by which additional external or "prior" information was worked into the GPR classification sequence. This produced "collaborative" processing such as would be achieved by pooling results or parameters extracted from data from another sensing mode, in addition to GPR. In the cases considered, use of external depth

estimates decreased the Pfa by about 15% to 30% without significantly affecting the Pd, provided that the depth information was accurate. In another test, as a handheld magnetometer preceded the GPR in the survey, the operator made crude determinations of obvious presence or absence of a magnetic dipole in the presumed target locale. When this information was pooled with the GPR parameters, it too improved performance, particularly in the resistant upper portion of the ROC curve (~ 90% Pd obtained at ~ 55% Pfa). Presumably the inclusion of more complete and sophisticated use of magnetometry (Mag) or electromagnetic (EMI) information would reinforce this result or amplify this trend.

It is difficult to make cost comparisons between the GPR system here and other discrimination technologies because 1) it is difficult to identify a "baseline" discrimination (as opposed to detection) technology; 2) the GPR technology being tested and consequent application techniques have developed rapidly during the course of the demonstrations and thereafter during this report's preparation; and 3) other, e.g., emerging discrimination systems often use contrasting approaches to analyze tests, often quantifying results in terms other than those applied here. Nevertheless, one can say that the initial capital cost for the GPR equipment as it existed at the time of the ultimate demonstrations is not great, as survey equipment goes (~ $37,000). The primary cost was and will be for labor in the field and during processing. The average number of hours of labor per target for all activities over all demonstrations, was about 0.7. Highly trained personnel often performed even the simplest tasks, given the prototype nature of the system and the importance of oversight during these tests. This translates into the equivalent of an upper limit of ~ $100 labor cost/target. At the same time, much less skilled and trained personnel were also used for these tasks with equal success. With proper training, even less skilled personnel could function as well, and some of the tasks have now been automated. Thus a reasonable estimate for future work might be less than $50 per target.

Emerging GPR systems can now cover a grid of points around a presumed target location in less time than the demonstration GPR required for its few linear scans over a target. Because of this speedup and the greater data and analysis resources it brings, it is a reasonable estimation that the emerging GPR survey and processing systems, including collaborative Mag/EMI data, should be capable of achieving the best of the "improved" performance examples shown below, without any greater cost than was required during these demonstrations. Lastly, there is no a priori reason to suppose that GPR discrimination should supplement Mag or EMI discrimination, as opposed to the other way around. While there are likely to be benefits from including GPR in multisensor surveying, what precedence to give to which aspects or parameters from which system will be case dependent, possibly target by target. In any event, it is unlikely that GPR will gain a prominent position for the straight detection part of surveying, except in distinct circumstances such as those with magnetic but relatively nonconductive soil/rock, or small, shallow, widely dispersed metallic clutter items.

While results in terms of certain criteria and in certain settings were uninspiring (e.g., Figure 4), in others they are strong (Figures 5 and 7). This means that the technology may merit use in instances where the kind of savings implied by the latter but not the former figures would apply. We do not in general recommend the application of our system in most circumstances at this time. This is because 1) in most (but not all) circumstances and with the most universal processing criteria (i.e., Figure 4, not Figure 7), the persistently missed detections limit

performance stubbornly in the upper portions of the ROC curves; and 2) the newer, much handier, faster, and cheaper GPR that has been developed will likely address the main performance limitations of the system demonstrated. While one cannot always delay application in anticipation of the next generation of improvement, in this instance we feel that the deficiencies in the old system and the capabilities of the emerging system warrant waiting.

2.0 TECHNOLOGY DESCRIPTION

2.1 OVERVIEW OF THE UWB, FULLY POLARIMETRIC GPR UXO CLASSIFICATION SYSTEM DEVELOPMENT AND ITS IMPLEMENTATION IN THE DEMONSTRATIONS

To demonstrate the UXO classification capability of the prototype GPR and to establish its performance baseline, the OSU-ESL teamed up with the lead institution, of USACE-ERDC, for a 3-year project supported by the Department of Defense (DoD) ESTCP. First, a broadband fully polarimetric GPR prototype was set up by the OSU-ESL with improved dual-polarization horn-fed bowtie (HFB) antennas. Although the network-analyzer-based prototype had the disadvantage of slow data rate compared to most commercial units, its ultrawide bandwidth (UWB) and fully polarimetric features could not be matched by any commercial GPR systems. Also, pending successful demonstration, the data rate could readily be improved (see below). This prototype was taken for blind classification demonstrations to test sites at Tyndall AFB, the Naval Research Laboratory (NRL) Blossom Point (BP) UXO Test Site, JPG, and the former Fort Ord. Details of the individual demonstrations, site characteristics, history, etc, are contained in references [7]-[11] and the references therein, e.g., [13]. At each site, the CRREL/Ohio State University (OSU) team collected GPR data locally around each flagged "hot spot," not knowing whether or not the spot contained a UXO. The flagging and decision as to which locations to flag were executed at each demonstration site by a field crew associated with the particular site, usually in consultation with ESTCP. In the last two demonstrations, these hot spots were chosen to resemble the locations that would be obtained from magnetometer or EMI surveys at live sites. In many cases, the flagging crew purposely introduced an offset between the known target location and flag location to simulate typical positioning uncertainty. In any case, all ground truth was closely held until after reporting of processing by the CRREL/OSU crew.

Data were collected between 20 MHz and 810 MHz in sandy soil (Tyndall and Fort Ord) or between 10 MHz and 410 MHz in lossy soil (wetter soil, engendering shorter relevant wavelengths at a given frequency and having a strong tendency to absorb the higher frequency radar signals: BP and JPG). UXO classification was done in post processing, after the team returned from the field. The first processing pass was generally completed overnight. Processing refinement for the less obvious cases was pursued later at a home base. In the ultimate form of the system, these blind classification results were prioritized according to target types (UXO-like or non-UXO) and confidence level (high, medium, or low). This information was then delivered to the ESTCP office, along with other estimated target features such as depth, length, and azimuthal orientation, for each measurement cell (flag locale). In detailed reports submitted for each demonstration after the ground truth had been provided, other summarizations of results were also included, such as ROC curves. The initial (blind) reporting usually took approximately 2 to 4 weeks after the field measurements. Sometimes the ESTCP staff and/or site crew released the ground truth in stages, for further performance assessment of processing strategies when some partial prior knowledge is available. As the project evolved, the system configurations, measurement approaches, data preprocessing techniques, feature extraction methods, classification rules, and performance assessment methods were refined and the improvements implemented. Data were examined for many more closely spaced positions along each antenna pass. Spatial and frequency patterns along each pass were also exploited.

In order to assess the GPR classification performance appropriately, two systems were employed. In the first, the default system, any object in the target list with a length-to-diameter (L/D) ratio greater than three was designated as UXO-like. This was the criterion applied to sort items within the ground truth list into UXO-like or non-UXO-like classes and was based on the notion that such items would have to be dug if *any* sensor system produced comparable shape/size information. Other available classification systems are based in effect on equivalent inferences, generally seeking evidence that an unseen target has a dominant scattering direction [14,15]. The radar signal processing does not directly produce an estimate of L/D. Rather, other parameters are extracted from the data and are examined to see whether or not they are likely to correspond to an elongated object. When the GPR parameters indicated that a particular target was UXO-like and the corresponding object in the ground truth list had an L/D equal to or greater than 3, this was viewed as a successful detection. If the GPR parameters indicated that an object was UXO-like by these criteria but in fact its L/D was less than 3, then this constituted a false alarm. In isolated instances, when some actual UXO at site were in fact not very elongated, a criterion of $L/D \geq 2$ was also tried to distinguish UXO-like from non-UXO in the ground truth.

To pursue this matter briefly, consider a key GPR signal feature in the classification system, namely the ELF. This is calculated from the eigenvalues obtained from the scattering matrix in the late-time response region. The ELF can have a value from zero to one, depending on the degree of linear polarization in the scattered field. A value of zero indicates complete rotational symmetry, i.e., $L/D \sim 1$ in all orientations, as for a sphere or other compact object. A value of unity indicates a long, thin object. Note that resonance information is implicitly included in this factor because the ELF is extracted from the "late-time" or "resonance" region of the time-domain responses. The resonant frequency also implies the length of the target (greatest linear extent in a dominant direction), and this is determined as an adjunct parameter. Like GPR, EMI and magnetometer systems respond to additional target features besides size and elongation, but in practice, discrimination approaches have had to rely on extracting the implication of only such basic features from the data. In particular, at present other discrimination systems typically just try 1) to estimate the overall size of the object and 2) to examine (in effect) dipole moments along different target axes, to ascertain the presence of a dominant direction as well as evidence that the unseen target is a body of revolution. Therefore, at best, the processing indicates that an unseen target has generic features associated with a UXO or class of UXOs, i.e., that it is UXO-like. If such Mag/EMI processing indicates presence of a target of UXO size and UXO proportions in terms of directional response, then such a target will unquestionably be placed on the "dig list."

Clearly, the approach here in using ELF and estimated target length (ETL) is not sufficient to separate a UXO-like piece of clutter from a TRUE UXO item of similar dimensions. However, the same can be said of Mag/EMI systems that likewise consider size and eigenvalues (directional dipole moment) ratios. Further, it was assumed that site managers would feel compelled to dig items that their survey and processing system deemed similar in overall size and proportions to UXOs sought. Thus, the UXO-like/non-UXO criterion seemed like a logical standard of comparison to other systems. This is tantamount to examining how well the systems do what they are designed to do. To a very considerable extent, the system here and alternative systems will succeed in identifying TRUE UXOs while using the UXO-like classification

criterion if and only if the competing clutter has substantially different characteristics from the UXOs. The GPR classification performance was evaluated and is reported according to *both* "TRUE UXO" and "UXO-like" sorting criteria, allowing readers to pursue their own notions in this regard, and to see the difference. These criteria are discussed further below.

After the first two demonstrations at Tyndall and BP, revised classification rules were adopted for the final blind tests conducted at JPG-V (Madison, Indiana) in June 2001 and at the former Fort Ord (Monterey, California) in October 2001. Two new measurement approaches were implemented to better simulate real-world scenarios and to improve the scan efficiency. First, a position error of size and direction unknown to the CRREL/OSU team was added to the actual global positioning system (GPS) location of the target. This was to reflect a more realistic situation in which each hot spot is most likely determined from Mag/EMI survey data. At real cleanup sites, the offset is probably not random but is related to the depth, size, and orientation of the UXO, given the characteristics of the Mag/EMI sensor systems used to locate "hot spots." Additional location errors may also be introduced by the positioning system used on the EMI/magnetometer surveying unit.

The second change in the measurement approach was to survey manually each flagged location using a Schonstedt Model GA-72Cd handheld magnetometer. This is the type of instrument commonly used by survey personnel during a mag-and-flag survey for an actual cleanup. This was done prior to the GPR measurements at the last two sites. A member of the survey crew generally had to precede the GPR unit to the next flag. The handheld Mag survey could easily be done more quickly than the GPR measurements and, as carried out, the Mag survey required no special skills. Therefore the addition of the Mag measurements had trivial impact on survey efficiency, cost, or throughput. As a kind of reality check, the Mag measurements provided a confirmation of the hot spot and also detected small near-surface clutter here and there. Equally important, sign change during the magnetometer sweep was sometimes clear enough to indicate the presence of a magnetic dipole pattern, as is associated with elongated targets inclined at some angle relative to the earth's field. If a magnetic dipole was observed, the approximate dipole orientation was then used as the orientation of the initial radar pass. The idea was to align as much as possible the primary copolarized GPR orientation with the principal target axis for maximum signal clarity. Other uses of this information for possible improvement of the GPR processing are described below. If a more accurate Mag survey map were to be provided by a previous survey, e.g. vehicular survey, the handheld survey would be superceded. Because of differences in the underlying physics, Mag and EMI tend to introduce opposing offsets into estimated target locations when those locations are based on maximum signal magnitude. Whether an offset from the ideal GPR survey position was introduced purposely by the site management crew or by real-time interpretation of our magnetometer readings, offsets placed a greater burden on accurate inference of azimuthal (horizontal angle) target orientation from the GPR data. Whenever the estimated target orientation (ETO) from GPR processing was clear enough to warrant it, at least one subsequent GPR pass was made in the ETO. This meant that a scan would still likely pass directly over the target (and through the optimal GPR view), despite an initial offset. However, poor initial ETO information combined with an offset of deeper targets could degrade performance.

It is revealing that classification performances were quite similar in the JPG-V and Fort Ord tests despite the very different environmental, UXO, and clutter characteristics. The soil at the Fort Ord site was mainly dry sand, which is generally very favorable for GPR. However, the very extensive tunnel networks created by small animals resulted in a high signal clutter level. These burrows and also the clustering of flags and presumably also of targets near one another reduced the signal-to-clutter ratio (SCR) significantly. The effect of all this on the data was that, while essential resonances frequently still showed through, ambiguities appeared in the ETOs. From this consideration, it is not entirely surprising to see Fort Ord classification performance similar to that obtained at the JPG site, where low SCR has repeatedly been observed in GPR studies. Notably, the crude handheld magnetic dipole detection at Fort Ord actually improved classification accuracy significantly, strengthening the case for a multisensor system.

2.2 FULLY POLARIMETRIC UXO GPR

The blind UXO classification demonstrations in this project were executed using the fully polarimetric GPR prototype developed by the OSU-ESL. The following sections provide brief descriptions of the radio frequency (RF) components, antenna unit, positioning and orientation instruments, and operation software. More detailed information can be found in the references, some of which are in the open literature, e.g., [8] and [12], with the greatest detail available in ESTCP project reports on the individual demonstrations [7]-[11].

2.2.1 RF Transceiver

The heart of the GPR system is a commercial vector network analyzer (VNA), model HP8712ET by Agilent, as shown in Figure 1. This device performs reflection and transmission measurements between chosen frequencies in steps of variable, i.e., specifiable size. The frequency increment was as little as 2 MHz and as great as 10 MHz. As a matter of definition, when a radar signal is transmitted and received from the same element *i*, "copolarized" data S_{ii} is obtained. If the radar signal is transmitted from element *i* and received by the orthogonal element *j*, "cross-polarized" data, i.e., $S_{ji,}$ is obtained. The particular VNA model we used could perform two kinds of reflection measurement in any single shot: 1) direct reflection measurement in the same polarization as was transmitted (S_{11}); and 2) measurement of cross-polarized transmission (S_{21}), i.e., measurement of reflection in polarization (E field orientation) #2 due to transmission in the orthogonal polarization direction #1. (See Section 2.2.2 for an explanation of antenna orientation and principal antenna directions.) The VNA could not measure S_{22} data (transmission and reflection polarization both in the orientation perpendicular to the principal antenna orientation, which was also the direction of travel). Therefore, a special RF switch box was built so the system could collect the fully polarimetric data, including S_{22}. Some newer models of VNA come with this capability; see manufacturer's information. By reciprocity, $S_{12} = S_{21}$, so it was not necessary to measure more than the three components—S_{11}, S_{12}, and S_{22}—to infer complete polarimetric data. Because both amplitude and phase were recorded for each of these three components, the scattering matrix can be rotated mathematically to obtain fully polarimetric information for any other set of principal antenna directions 1 and 2 without physically rotating the antenna itself about an axis normal to the ground.

Figure 1. Vector Network Analyzer (HP8712ET).

2.2.2 Antenna Unit

An UWB fully polarimetric HFB antenna is the key component of the whole system. Such an antenna element needs to be able to operate over a wide frequency range (10~810 MHz) to cover the resonant features of most UXO sizes in most soil types. An HFB antenna is composed of a dielectrically loaded transverse electromagnetic (TEM) horn section and a resistively terminated bowtie dipole section, as illustrated in Figure 2. This horn section is detachable such that horns with different dielectric constants can be used. This can produce a better match with the dielectric constant of the ground, in turn providing better sensitivity. Two linearly polarized HFB elements are arranged perpendicular to one another, as shown in the figure, to provide the two orthogonal send and receive channels. Each element can be configured to operate in the transmitting or receiving mode. By recording all the S_{11}, S_{22} and $S_{21} = S_{12}$ data at a given position, the polarization of the scattered field from the target observed at the antenna plane can be obtained. This polarization information can then be used to infer the UXO orientation projected onto the plane of antenna aperture.

Because the target orientation was estimated with respect to the antenna orientation, a digital compass was attached to the mounting structure of the antenna. This was recalibrated at each test site. For positioning along each scan line, some initial position relative to the apparent target location was ascertained. Then, marks on the front wheel of the towing vehicle were aligned in succession with a reference on the vehicle frame, providing a measure of the vehicle's advance between shots.

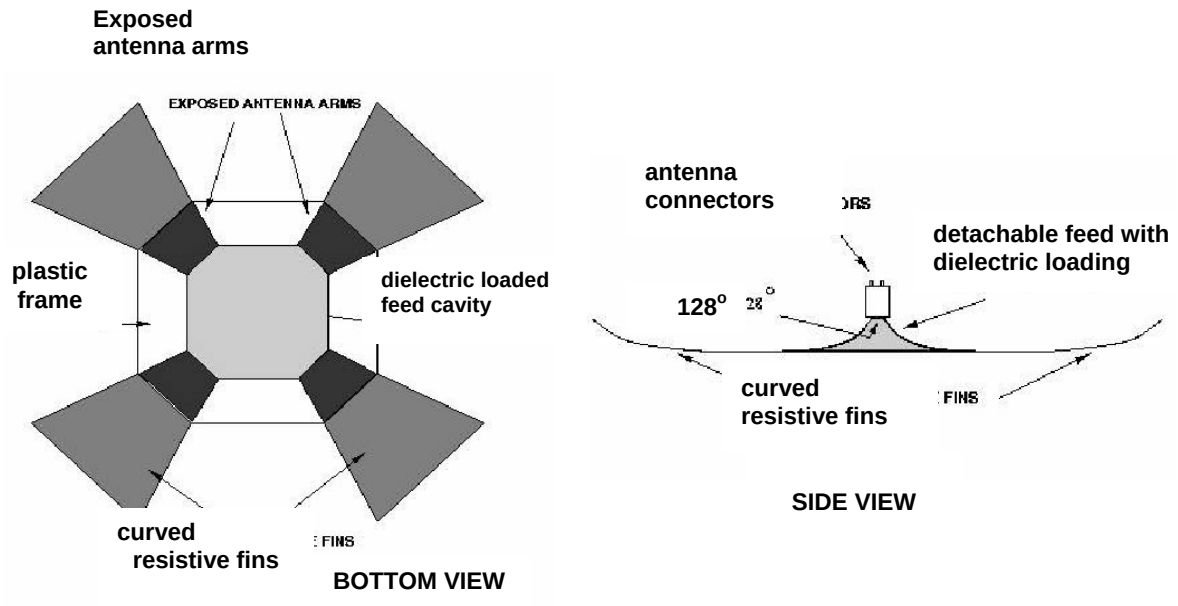

Figure 2. Diagram of the Bottom View and Side View of the OSU-ESL UWB Full-Polarization GPR Antenna.

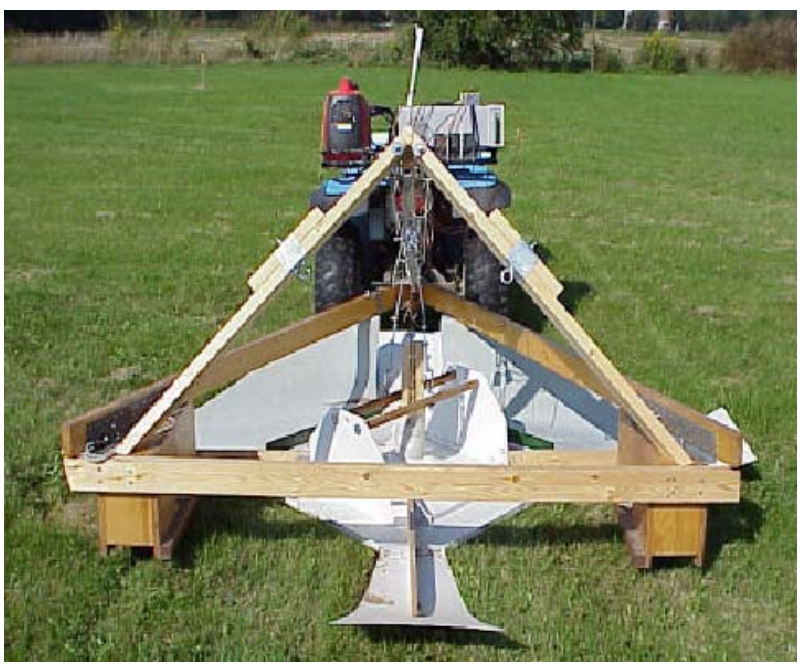

Figure 3. UXO GPR Configuration Used at Blossom Point, JPG, and Fort Ord Sites, with Antenna Arms Aligned with and Perpendicular to the Travel Direction.

3.0 DEMONSTRATION DESIGN

3.1 PERFORMANCE OBJECTIVES

The overall objectives of the demonstration series were

- To show what, if any, the capabilities of this GPR system are for discriminating buried UXO from clutter
- To quantify that discrimination capability as a function of environmental conditions, UXO and clutter types, and processing approaches
- To compare whenever possible our GPR's discrimination capabilities with those of other baseline technologies
- To estimate cost and cost savings from using GPR for UXO discrimination
- The performance specification developed by the group will define the operational requirements of any future digital-imaging-based opacity determination system.

These overall demonstration objectives might be translated into primary and secondary performance objectives:

- *Primary.* Achieve quantified discrimination capability that is better than arbitrary or random classification of anomalies that have been identified by other means, e.g., Mag, EMI surveys, or other records
- *Secondary.* Achieve quantified discrimination capability that is better than that of established or baseline UXO discrimination technologies.

Discrimination performance is quantified here in terms of Pd and Pfa; and in turn the relation between Pd and Pfa is examined in terms of the [misnomer] receiver operating characteristic or ROC curves. These terms are defined above. As used here, "showing some discrimination capability" means producing a more successful UXO/non-UXO classification or consequent dig/no-dig judgment than random or arbitrary classification of anomalies, as reflected in ROC curves. This is explained further below.

We speak here of the "UXO class" and "non-UXO class" instead of simply "UXO" and "non-UXO" because, as observed above, essentially all processing known to us of sensor output for UXO discrimination proceeds effectively in those terms. That is, it seems that no currently viable system succeeds in identifying a concentration of explosive within a metal projectile enclosure. Nor can any of the systems identify a UXO in the manner that, say, medical imaging can sometimes produce detailed, realistic pictures of structures and composition of items of interest. Rather, at present one must ascertain whether a signal anomaly corresponds to the type, size, and shape of metal object associated with UXOs that could be at a particular site. Under this criterion, if the processing and classification criteria identify such objects as being in the UXO class, one considers these to be successful detections, whether they are TRUE UXOs or not. The discussion surrounding this classification system notwithstanding, we note that the use

of UXO-like or TRUE UXO ground truth sorting criteria had little impact on our recommendations for future implementation.

3.2 SURVEY, PROCESSING, AND INTERPRETATION METHODS

This section briefly describes the algorithms developed for processing the UWB, fully polarimetric GPR data and for extracting the target features, including linearity, depth, length, and orientation. More details appear in Appendix B and in the reports and papers in the references [7]-[12].

3.2.1 Measurement Approach

The measurement approach was finalized after the second demonstration. For each target locale, the GPR made a minimum of two passes, in two or three stages, in orientations parallel and transverse to the ETO. Prior to the GPR measurements, a conventional Schonstedt magnetometer was used to manually survey the local area near the flagged "hot spot" to determine the maximum magnetic response position and to check for the existence of a magnetic dipole (sign change in magnetometer reading or double-peak output in magnitude-only unit). A magnetic dipole response pattern indicates an elongated ferrous object. If a magnetic dipole was detected, the initial radar pass was then directed along the estimated orientation of the dipole, projected onto the plane of the ground surface. That direction provided an approximate indication of the ETO. If no dipole was detected, an arbitrary orientation was chosen for the initial pass. The radar data collected from the first passes was processed on site and/or overnight to determine an ETO of any target that showed high linearity (high ELF). If the orientation estimated from radar data was close to that from the magnetometer, then the second pass was oriented perpendicular to the orientation of the first pass. If the ETO from GPR processing was significantly different from the apparent magnetic dipole orientation, the second and third pass would be chosen to be parallel and perpendicular to the new orientation found from GPR data.

If GPR data collected from the first pass showed that the maximum GPR response appeared to be offset from center of the GPR scan, i.e., flagged position, the second pass would be centered at the position where maximum GPR response was observed in the first pass. From the JPG-V test, it was found that the orientations of 41 out of 72 UXO-like items were either approximately parallel or perpendicular to the scan directions predicted from the magnetic dipole, as used to guide the first pass. This certainly significantly reduced the number of passes required, compared to the number that would have resulted from a randomly picked first orientation. Magnetic dipole orientation estimated from a more sophisticated mapping system should be more accurate and efficient then the current Schonstedt-waving approach.

3.2.2 Preprocessing GPR Data

The purpose of preprocessing the GPR data is to improve the signal-to-noise ratio (SNR) and SCR, thereby improving the accuracy and stability of feature extraction. Typical GPR data contain system and environmental noise that limits the ultimate sensitivity of the system. However, because the clutter level is usually much higher than the noise level, it is the SCR that almost invariably determines the detection sensitivity in our GPR measurements. A detailed treatment of this is provided in our report on the results of the BP demonstration [9]. GPR signal

clutter can come from ringing within the antenna itself or reflection from the contact between the antenna and ground surface. Subsurface inhomogeneities due to variations in water content, soil composition, and natural features such as voids, roots, and rocks also produce signal clutter. Each type of clutter has its distinguishing features that may or may not be similar to the signal content from a UXO. Most natural clutter does not have strong electromagnetic resonance. It also typically lacks linearity, exceptions being some of the ditches or animal tunnels we encountered in these demonstrations.

In most GPR applications, the major clutter source is the antenna itself, e.g., when there are impedance mismatches. Also, for UXO classification it is essential to have little or no ringing or polarization distortion from the antenna. These problems had to be addressed in antenna design because they are difficult to remove or calibrate out using processing procedures. In the absence of distorting environmental features, the innovative antenna system used in these demonstrations showed outstanding suppression of ringing and good polarization quality. Thus any troublesome resonance and polarization distortions generally resulted from environmental features.

3.2.2.1 Ensemble Background Subtraction

In the raw copolarized responses, S11 and S22, strong antenna clutter is present due to the reflection at the antenna feed point. For the HFB antenna, this reflection level is approximately 20 dB over most of the frequencies. For a broadband antenna, this value is considered excellent. It is very difficult to achieve a reflection level lower than -30 dB for the kind of bandwidth and frequency content considered. However, for the specialized purposes here, this level is still intolerable. Because of soil losses and geometrical spreading of the radar beam, signal strengths from many buried targets of interest will be weaker than -20 to -30 dB. Because the HFB is specially designed to produce a fairly uniform reflection at the feed point independent of the content of any particular measurements, this antenna clutter can usually be reduced further by 30 ~ 40 dB via background subtraction. A common practice is to calculate the average waveform from all the waveforms collected in one scan and then to subtract this average waveform from the data. The underlying assumption is that the background is omnipresent and smooth and will emerge in the averaging, relative to any discrete target. All the data discussed or presented in this document have had the background subtracted.

3.2.2.2 Data Calibration

A system calibration was also performed to remove any distortion related to the RF system and cables leading to the antenna. This was done by measuring standard loads such as a short or a matched load placed at the end of the cables. In addition, a field antenna calibration procedure was performed. The purpose of these calibrations is to obtain true target responses as if the incident field had a flat spectrum. The field method measured the backscattered responses of a very long conducting cable wire laid on ground surface beneath the antenna, at 45° with respect to the antenna arms, such that the ends of the wire extended very far beyond the edges of the antenna. The background data in the absence of the wire was subtracted to obtain only the wire response multiplied by the antenna's transfer function. Because such a thin, long conducting wire has a very smooth response spectrum, any large variation in the spectrum can be identified as coming from the antenna. The long wire calibration procedure had the significant advantage

that it automatically included the effect of soil near the ground surface. It was repeated when soil conditions changed significantly.

3.2.2.3 Adaptive 2-D Spatial Smoothing

In GPR scan profiles as conventionally displayed, a discrete object produces a reflection record roughly in the form of a hyperbola, with tails pointing downwards. The peak of the hyperbola is located at the position in the scan where the antenna was closest to the target. Objects at different depths and locations will produce contrasting hyperbolas. Therefore a preprocessing system was designed in which the operator identifies a hyperbola that appears to correspond to the target. Then this hyperbola shape is used as an averaging trajectory over the whole profile, suppressing signals that do not conform to the hyperbola of interest. The effectiveness of this technique for bringing out signals of interest relative to clutter is illustrated in the project final report [see www.estcp.org] and in the individual demonstration reports listed in the references.

3.2.3 Feature Extraction

Appendix B provides some details of signal feature extraction methods, with more details in the individual demonstration reports and published papers [7]-[12]. Here the most important parameters that were extracted are reviewed; it was on these that the classification processing was based.

- *Estimated target depth*. This is determined by measuring the time delay between the ground surface signal and the earliest return from the target of interest. Both length and depth estimation must to be done in conjunction with a proper estimation of soil electrical properties, which were measured using an OSU soil probe.
- *Electromagnetic complex natural resonance (CNR) and ETL*. When a radar beam strikes an elongated metallic object, electric currents are set up that oscillate back and forth around (transverse to) its primary axis and also parallel to the main axis [5]. Each of these has preferred natural frequencies, or resonances, that produce peak signal magnitudes. For elongated objects, the transverse resonances are relatively weak and tend to die out early in time, during which they are often entangled with strong clutter. The longer lasting, lower frequency late time axial resonances are therefore preferentially sought out in the processing, despite the fact that signal magnitude typically diminishes greatly by late time. The presence of such a late time resonance in a clear orientation (polarization) is indicative of an elongated object. The peak frequency of the CNR allows the processing to determine the ETL, given the soil parameters mentioned above.
- *ETO and density (DEN) of signal about that direction*. Given the fully polarimetric nature of the scattering matrix obtained by our system, it can synthesize equivalent scattering matrices for all possible polarizations. The dominant polarization orientation indicates the ETO, and the density of the signal around that dominant orientation is a measure of the clarity of that determination.

3.3 UXO CLASSIFICATION RULES

Once the signal features and extracted parameters described above are obtained, they are fed into the classification system. This is a set of rules designed to discriminate UXO-like items (usually L/D ratio greater than three) from other metallic objects. The system is described in more detail in Appendix B and in the individual demonstration reports and published papers [7]-[12]. It is based predominantly on late-time polarization features (ELF and ETO) as a function of antenna position and scan orientation. Several rules involve qualitative spatial pattern recognition. All characteristics in the qualitative descriptions that are sought "by eye" can be shown to have a solid physical basis, based on rigorous numerical model simulations [20]. Further, recognition of the essential features has been automated during work following this project [see the appendices of this project's final technical progress report, www.estcp.org].

This page left blank intentionally.

4.0 CLASSIFICATION PERFORMANCE

The GPR UXO classification performance based on the above rules and parameters is summarized briefly here. The results presented focus on the blind tests performed at the most recent JPG-V and Fort Ord sites, after the final classification rules were adopted and the manual magnetometer survey accompanied the GPR. Detailed analysis of the classification performance and causes of errors for all blind tests (Tyndall, Blossom Point, JPG-V and Fort Ord) are available in the individual ESTCP reports [7], [9]-[11].

4.1 BASELINE PERFORMANCE

Figure 4 shows the UXO classification ROC curves from blind JPG-V and Fort Ord measurements based on TRUE-UXO criteria. This means that even a piece of metal with geometry similar to a UXO was considered to be in the non-UXO class in the ground truth. The curves shown were obtained based on the following six judgment thresholds:

(1) UXO with HIGH confidence
(2) UXO with MEDIUM confidence
(3) UXO with LOW confidence
(4) CLUTTER with LOW confidence
(5) CLUTTER with MEDIUM confidence
(6) CLUTTER with HIGH confidence.

The confidence levels were established based on the following qualitative observations:

- HIGH—good SCR, clear scattering patterns, clear ETO
- MEDIUM—medium SCR, discernible scattering patterns, at least identifiable ETO
- LOW—low SCR, ambiguous/insufficient/unfamiliar scattering patterns, unstable/ambiguous ETO.

Application of the second threshold, for example, classifies any item as UXO that has a medium or high confidence level as a UXO. All other items are classified as clutter. While one can say that the processing shows some definite discrimination capability, producing lines above the 45° "LOND", the performance is not inspiring. If the "UXO-like" criterion is adopted, the ROC curves in the right plot result, where "LD2" and "LD3" indicate whether the "L/D>2" or "L/D>3" criterion was adopted for target sorting in the ground truth. More than 50% of UXO-like items were correctly classified with 90% of clutter items rejected based on the top judgment threshold (1)—UXO with high confidence. Unfortunately, the classification rate rises only slowly thereafter as the thresholds decrease.

It is notable that similar classification performances were obtained from both test sites despite the very different environmental, UXO, and clutter characteristics. While the Fort Ord site contains mainly dry sand, the very extensive badger tunnel networks resulted in high clutter levels. Often targets were clustered as well, so that more than one appeared within the sensor's

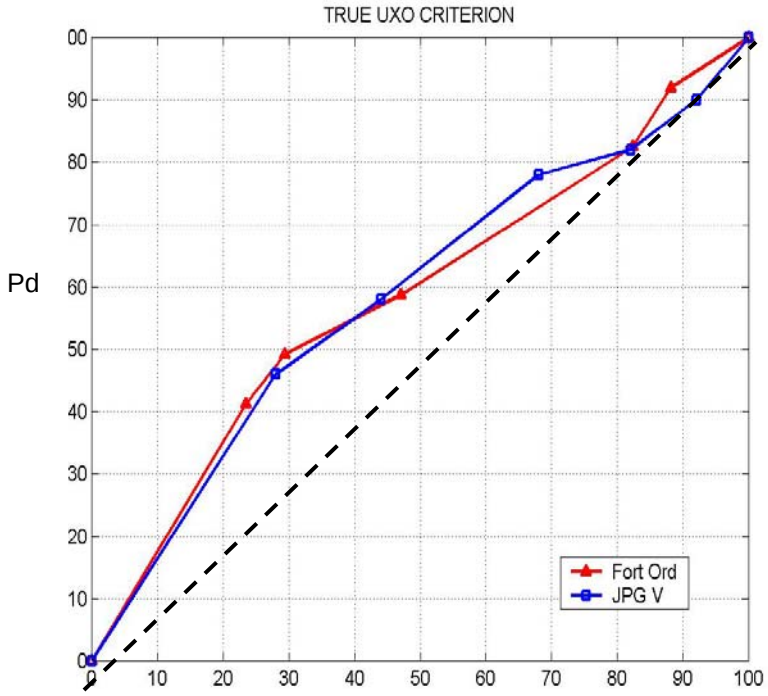

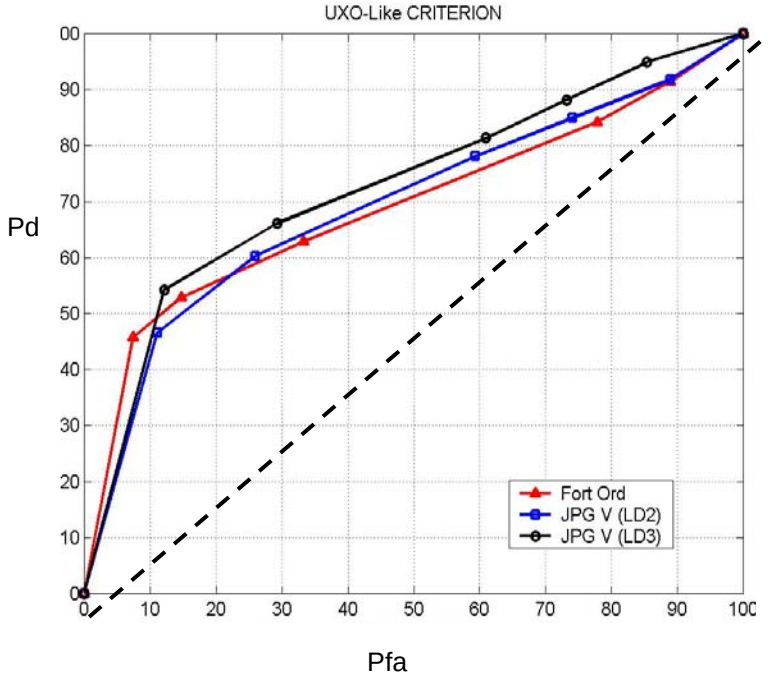

Figure 4. Classification ROC Curves Based on TRUE UXO Criterion and on UXO-LIKE Criterion with Dashed Line of No Discrimination.

footprint at the same time. Thus it is comprehensible that the classification performance was similar to that at JPG, where the soil conditions are well known to produce low SCRs in radar applications.

4.2 PERFORMANCE IMPROVEMENT

The measurements at Fort Ord contain an unusual number of UXO and UXO-like items with good resonance and linearity but ETOs that vary significantly between passes in different orientations. This caused them to be declared as non-UXO items during the blind classification. Thus in cases where the first GPR pass had a significant offset from the target, large ETO and position errors often affected the rest of the scans. The ETOs obtained from the all the passes represented target orientations observed from different oblique directions, as was not intended for the processing. At the same time, the majority of these missed UXO items did indeed show magnetic dipole patterns during the manual magnetometer survey, as noted in our field logs. This prompted us to investigate the inclusion of the presence of magnetic dipole pattern in the classification processing. Table 1 shows the rule adopted for upgrading the classification based on the apparent presence of a magnetic dipole, regardless of its strength. Figure 5, left, compares the ROC curves before and after inclusion of the magnetic dipole criterion. A significant improvement in the correct classification rate is achieved, particularly in the upper reaches of the ROC curve, where approximately 90% Pd is attained with approximately 50% Pfa.

Table 1. Rule for Class Upgrade When Magnetic Dipole Is Present (1 = UXO)**.**

Original GPR ID	GPR Confidence	ELF Values	Upgraded ID	Upgraded Confidence
1	H	0.7~1.0	1	H
1	M	0.7~1.0	1	H
1	L	0.5~0.7	1	M
0	L	0.7~1.0	1	M
0	L	0.5~0.7	1	M
0	LMH	0.0~0.5	1	L

In examining the classification performance for the BP demonstration, we noted that many of the missed targets were relatively deep in the very lossy soil. Thus the signals from the target were quite faint, and the processing focused erroneously on stronger reflections from near-surface soil disturbances. In a sense, the discrimination algorithm operated correctly in that it reported that these signals did not correspond to UXO. However this resulted in a reduced Pd. We speculated that this kind of problem could be alleviated by inclusion of depth estimates from some other sensing mode. Mag has been used to constrain assumed depths in EMI processing, e.g., [16], and similarly Mag/EMI or other estimated depths can be used in the GPR processing. Figure 5, right, shows ROC points for JPG, i.e., discrete Pd/Pfa ratios obtained from the processing. The points labeled EMI correspond to data we were furnished from other JPG-V classification tests using EMI equipment. Round 1 shows results obtained from GPR data alone. In Round 2, the GPR processing also referred to the estimated depth information. In Round 3, the GPR processing again referred to depth information but used the most accurate information possible i.e., ground truth values. While the EMI-estimated depths did not affect results very significantly, the ground

truth depths moved the results into a lower false alarm range without appreciably lowering the detection rates. This indicates that the GPR performance can be improved significantly by depth indications from other sources, provided the information is of high enough quality.

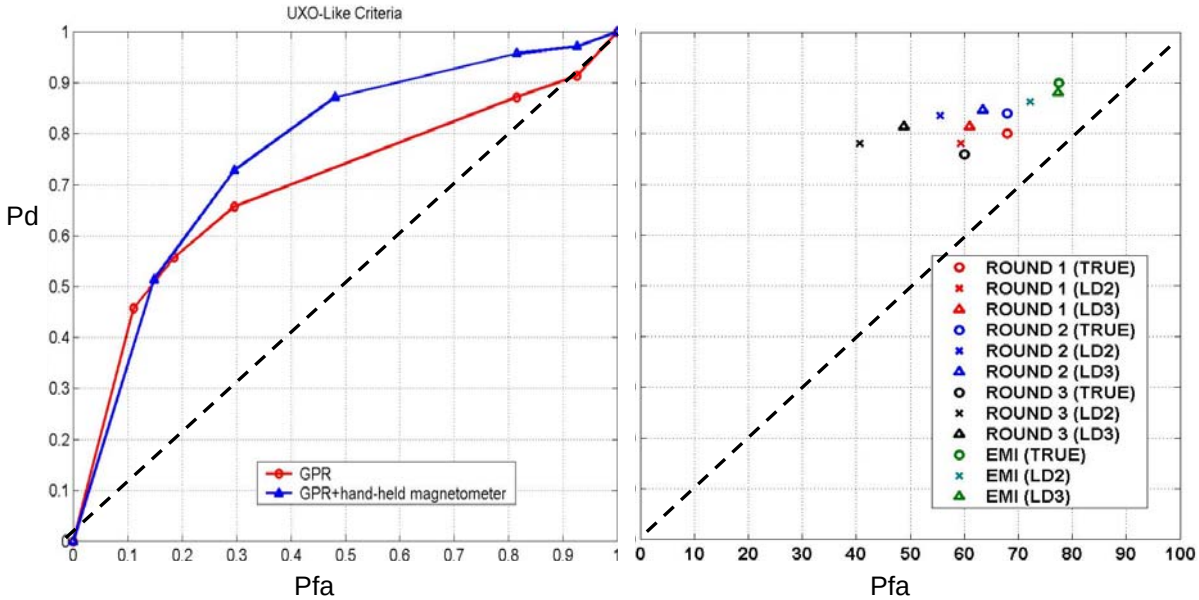

Figure 5. ROC Curves for Fort Ord Showing Performance Obtained from GPR Alone and Improvement from Inclusion of Mag Dipole Presence as a Factor (left) **and ROC Points from Different Rounds of Processing at JPG-V using TRUE-UXO, LD ≥2, and LD ≥3 Criteria** (right)**.**

Other target features that can be useful for improving UXO classification are produced in the course of the processing. Figure 6 plots the absolute error of the estimated length and depth for UXO-like items that were correctly classified. The correctly classified items were used because incorrectly classified items often constituted cases with poor SCR, poor CNR (needed for length estimation) or other data incoherence, so that no length or depth estimation would reasonably be credited to those cases. Most of the length error is less than 10 cm, and most of the depth error is less than 20 cm. Note that these results were obtained only from blind GPR processing results. The length values tend to be overestimated because of the additional propagation distance of the induced currents on curved body and over the fat ends of some UXOs. In another layer of processing, one could compensate for this, so that the error distribution was more nearly zero mean. The depths also tend to be overestimated possibly because of the bandpass filtering. This could be improved by selecting the time position of the surface reflection after the bandpass filtering has been done.

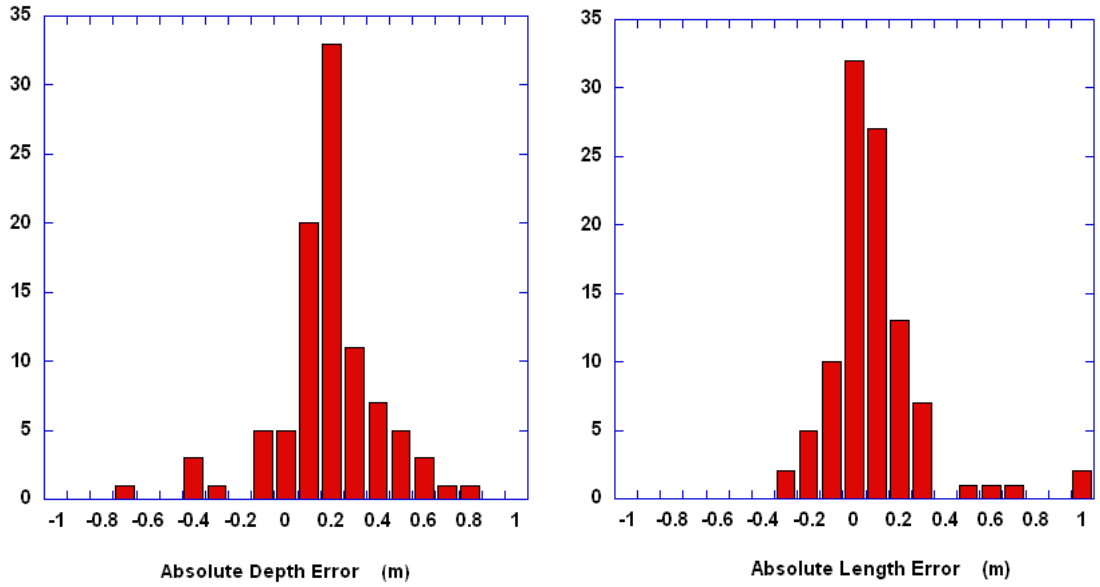

Figure 6. Based on JPG-V and Fort Ord-GPR Data Alone, for Correctly Classified UXO-Like Items: Absolute Depth Estimation Error (left) **and Absolute Length Estimation Error** (right)**.**

Other UXO discrimination systems attempt to infer much the same thing as ours, in the sense that parameters are evaluated to infer the general shape of the unseen object. By contrast, others seek signatures of specific targets, based on information that certain types of ordnance may be found at a particular site—the spectral "fingerprinting" or pattern matching approach. In a step towards the second approach, we find quite good classification performance in some test cases pursued at the Tyndall site. While we concentrate here on the later demonstrations for which the survey and classification system had matured further, at Tyndall there were large enough numbers of particular targets to warrant construction of ROC curves for individual items. Figure 7, left, shows ROC curves for the 105 mm projectiles buried at Tyndall, obtained when the usual decision criteria were applied together with a judgment as to whether the ETL agreed with that for the target sought. Thus the classification system asked the questions: 1) Is this item UXO-like? and 2) Is its length within some specified tolerance relative to that for the particular UXO sought? The different ROC curves in the figure correspond to different tolerances of length error relative to that of the 105 mm. In actuality, tolerances were applied to the CNR peak frequency, which is inversely related to the electromagnetic wavelength and hence the ETL. Thus a 50% peak frequency tolerance translates into acceptance of lengths between 2/3 and 3/2 that of the catalogued length. With this additional classification criterion, performance is quite good, reaching a 100% Pd at a 40% Pfa.

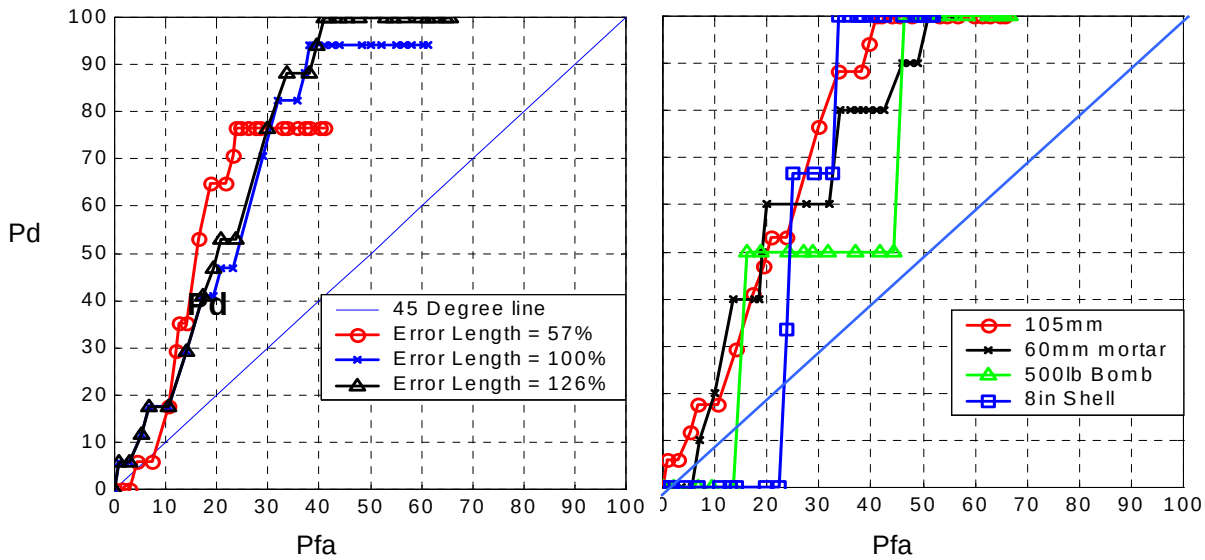

Figure 7. ROC Curves for the Tyndall Site for Various Ordnance Types, Obtained When ETL Was Included in the Criteria for 105 mm Projectiles of Different Length Error Tolerance (left) and for Various Ordnance Types with Sufficient Length Tolerance to Reach 100% Pd (right).

Treatment of other UXO types also fared well under processing with this additional criterion. The plot on the right in Figure 7 shows ROC curves obtained in this manner for other targets as well as for the 105 mm, using length tolerances sufficient to achieve a 100% Pd. The curves necessarily proceed in gross steps when only a few of some ordnance types were present, perhaps better viewed in terms of ROC points at the left edges of the large steps. In any case, clearly the trend is towards good performance, with a 100% Pd and a Pfa between about 35% and 45%.

4.3 ANALYSIS OF PERFORMANCE

The baseline performance in the last two focal demonstrations is shown most succinctly in the ROC curves of Figure 4. When asked to identify TRUE UXOs in the target set, the system produced results consistently above the LOND, but not greatly. The system clearly does much better when asked to do what it was designed to do—detect the presence of objects with proportions like those of UXOs (UXO-like criterion). Particularly for the purposes of comparison to other sensing systems, the UXO-like criterion seems most appropriate, partly because ascertaining UXO-likeness in signal parameter patterns is what almost all other systems do. Other systems and the one treated here will do better when clutter is very different in form from a UXO and will do worse when it is not. This makes it particularly difficult to compare tests that involved differing target sets. Favoring this criterion also follows the guidance of field personnel from the Huntsville Center who have stated repeatedly that, if a surveyor indicates that an object is the size and shape of a UXO that could be present, they will dig it up regardless of

what else the processing indicates. This has also been cited to us as a legal requirement (Dr. Anne Andrews, personal communication).

An effort was made to seek sites with very different environmental conditions to see the dependency on soil type and state. However, despite the very considerable physical and target set differences between these last two sites, classification performance was quite similar. Unfortunately, this probably does not reflect some consistent character or capability in the surveying and processing. Rather, countervailing influences more or less "cancelled out" in the Fort Ord test, where dry sandy soil was very favorable to GPR but signal clutter from animal burrows and the clustering of targets was not. Because postprocessing analyses indicate that the performance at Fort Ord was clutter limited, one can speculate that better performance would be seen under similar soil conditions and target set but without the subsurface clutter sources. Nevertheless, the level of performance observed under a diversity of conditions does support the view that one is likely to achieve roughly comparable performance at other sites.

Performance was limited both by false alarms and especially by missed UXOs.

Causes of false alarms:

(1) Ground scattering from formations that had linear features such as trenches, directional depressions, or animal tunnels

(2) Small vertical plate-like scrap

(3) Scrap with thin extended parts (curved or non-curved).

Causes of missed UXO-like items:

(1) Copolarized channels for targets of small sizes and depths contaminated by the scattering from subsurface layers and inhomogeneous medium

(2) Processing focus on incorrect depth, i.e., faulty late-time identification

(3) Weak or absent target responses due to large depth, steep inclination angles, and soil absorption

(4) Large target position offset, in turn possibly due to linear features as in (1) above.

Incorporating information in the GPR processing from manual (untrained) Mag surveying improved the GPR measurement procedures and subsequent processing. Particularly because the Mag information was so crude, this suggests that exploitation of more sophisticated Mag/EMI data might improve GPR performance rates beyond the best cases shown above. Prior or external depth information improved GPR classification performance, provided that it was accurate. The specific level of accuracy required in depth estimates to achieve a given GPR classification performance improvement is as yet unknown. Depending on the particular ground truth sorting criterion used, use of depth guidance to enhance the GPR processing led to Pfa reductions from

values greater than about 60% to something above 40%, without appreciable decrease in detection.

4.4 PERFORMANCE COMPARISONS

It is difficult to compare the GPR discrimination performance here with that of other systems because 1) there are few other discrimination systems; 2) others are generally considered different situations, operating with other technologies, objectives, criteria, and/or analytical frameworks; and 3) results were often reported in terms such that they are not comparable to the ROC curves here, e.g., using false alarm count as opposed to Pfa. These differences notwithstanding, a few highly approximate comparisons follow for the sake of the perspective they may offer.

EMI is usually regarded as the most promising UXO discrimination tool. EMI discrimination processing to date has usually inferred principal magnetic polarizability values ("∃" values) of an unseen target, and from those has judged whether the object is UXO-like or not. A matched filter approach based on these ∃ values produces ROC points in ESTCP Project UX-9918 [15]. For JPG area 1 the raw Pd reported was 67% with a Pfa of 80%; however, this position below the LOND was largely due to undetectability of small 20 mm UXOs. When the 20 mm are discarded, the Pd is about 88% versus a Pfa of 80%, which is above but quite near the LOND. In a similar pattern, for JPG area 3 the cited project shows an ROC point slightly below the LOND when the 20 mm are included, and a ROC point of Pd 94% versus Pfa 83% when the 20 mm are excluded. These are comparable to the performance shown here under various options. However, the comparison is not very illuminating in that these points are only in the high Pfa, high Pd region where most ROC curves must converge, on the upper right corner of the plot. The best performance here, in Figure 5, is clearly superior to those in the cited project. However, it is unclear how performance in the other project might have improved if they had used the UXO-like criterion. Basically, the proximity of their best ROC points to the LOND is probably a consequence of 1) the aim of achieving a high Pd and 2) the fact that, like essentially all other discriminating processors, they have used a classification system based on UXO-likeness in extracted parameters but scored detections based only on the TRUE UXO criterion.

In a Mag and EMI sensor fusion project (ESTCP-9812), ROC curves in terms equivalent to Pd and Pfa are shown [14]. Figure 8 is reproduced here from that reference with a dashed LOND added. ROC curves for three methods are shown for the L Range Demonstration. One, based on Mag size, is deemed comparable to the discrimination that the Multi-Sensor Towed Array Detection System (MTADS) (see numerous references via www.estcp.org) could produce for this site, based on Mag alone but with reference to a calculated magnetic dipole size. Curves from two other methods are also plotted, including results in connection with the sensor fusion system in the demonstrations. The baseline (red) curve deemed representative of MTADS Mag treatment alone is of roughly the same quality as the baseline case here in which the TRUE UXO criterion is used (Figure 4, left). The main difference is slightly stronger performance in the approach here at the lower Pfas and worse performance at the higher Pfas. The baseline performance curves here using the UXO-like criterion with depth feedback (Figure 4, right), are much stronger than any of the cases in Figure 8 in the lower Pfa range but, again, weaker in the upper Pfa region. The improved ROC curves shown above for Fort Ord, based on the UXO-like criterion with inclusion of Mag dipole presence as a factor, are comparable to the strongest

curves in Figure 8. Of course, one cannot say how much the curves in Figure 8 would change if the investigators had also used the UXO-like criterion.

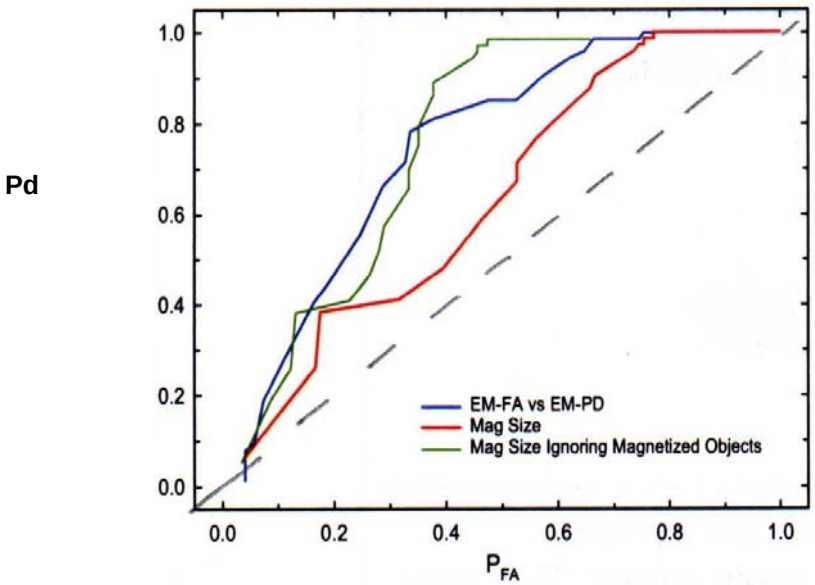

Figure 8. MTADS Discrimination Using Mag Data Alone (red); Enhanced Results Obtainable from MTADS Mag Data, Including Mag Dipole Orientation Information (green); and Results Including Information from "three β" EMI Data (blue) (ESTCP).

This page left blank intentionally.

5.0 COST ASSESSMENT

5.1 COST OF THE DEMONSTRATIONS

Tables 2 and 3 show the demonstration costs, first in terms of labor and human activity (Table 2) and then in terms of equipment costs (Table 3). In the former, "target" as in "number of targets" simply indicates a surveyed location, whether a UXO, non-UXO, or any target at all was present. In terms of throughput, on average about 24 min per target was required for the actual GPR scans, with very little variation across the sites. While more data were collected in the later surveys, efficiency was also greater. The GPR systems developed following this project [17] would be able to cover ground at a slow walking speed. If one considers a "slow walk" to be ~ 20 ft/min, and assumes 5- to 10-ft grid lines at 1-ft spacing, that implies about 1- to 5-min/target actual survey time with the new GPR, not including transition time between target locales. Also, because the newer units are small, light, and inexpensive, a number of them could be operated in parallel at any particular site.

Table 2. Labor and Activity Costs of the Demonstrations.

	JPG	Tyndall	Fort Ord	BP	Hour/Unit
Number of targets	100	152	97	87	
Number of GPR scans	243	365	242	209	0.1667
Number of Mag scans	100	0	97	0	0.0333
Soil property measurements/day	1	1	1	1	0.5
Target data processing sequences	243	365	242	209	0.0833
Equipment setups/day	1	1	1	1	0.5
Labor hours for:					
GPR scans	41	61	40	35	
Mag scans	3	0	3	0	
Soil property measurement	3	4	3	3	
Data processing	20	30	20	17	
Equipment setup	3	4	3	3	
Total labor hours @ each demonstration	70	99	70	57	
Labor hours/target	0.70	0.65	0.72	0.66	
Overall average labor hours/target	0.68				

Table 3. Equipment Costs of the Demonstrations.

Network analyzer	$11,512	1	$11,512
Generator	$500	1	$500
Notebook computer	$5,000	1	$5,000
Antenna	$15,000	1	$15,000
Tractor	$1,500	1	$1,500
Frame	$1,000	1	$1,000
Switching box	$500	2	$1,000
Etc.	$2,000		$2,000
Total equipment cost			**$37,512**

5.2 COST COMPARISONS AND POTENTIAL SAVINGS

It is difficult to make cost comparisons between the GPR system here and other discrimination technologies. This is because 1) it is difficult to identify a "baseline" discrimination (as opposed to detection) technology; 2) the GPR technology here and consequent application techniques have developed rapidly during the course of the demonstrations and thereafter during this report's preparation; and 3) other emerging discrimination systems, e.g., used different analytical renderings to treat cases that were different from those here, often quantifying results in other terms. Nevertheless, one can say that the initial capital cost for the GPR equipment as it existed at the time of the ultimate demonstrations was not excessive. While the newer equipment referenced above might cost only about $5,000 to $10,000, compared to the $37,000 expended in these demonstrations, one might use $15,000 in estimates to account for maintenance, replacement, and upgrades. In any case, the primary cost did and will reside in man hours in the field. As noted above, using the costs in these demonstrations as a guide indicates a labor cost of between ~ $50/target and ~ $100/target, depending on the level of training and professional qualifications of the personnel. There is no reason that systematic implementation could not be carried out ultimately with less highly trained personnel than even the least skilled who were used here. This together with the faster, handier GPR systems could drive the cost well below $50/target.

Potential savings from the demonstrated GPR technology can be estimated only very approximately. Consider an overall average cost per dig to be ~ $200 (Roger Young, Huntsville Center, personal communication). Many sources attest to the fact that at most actual UXO cleanup sites, many, many more non-UXO items are dug up for each UXO that is excavated. Many were not approached as potential UXOs while being excavated, that is, they were recognized as clutter and presumably removed without the care and attendant cost devoted to a potential UXO. Regarding only the "serious" digs, then, consider the situations in which results such as those in Figure 7 might be expected. The very high number of digs executed in real cleanup is driven by the determination to achieve near 100% detection. In the aforementioned figures one sees ~ 100% Pd at around 40% Pfa. Optimistically then, under the assumed conditions, about 60% of the false alarms in serious digs could be avoided by using the demonstrated GPR technology. Even given the constraint that the conditions warrant reference to these ROC curves (favorable, i.e., dry, relatively homogeneous soil, distinct target types, etc.), this is optimistic primarily because it assumes that at a real site the density of metallic clutter

would not degrade performance below what appears in the figures. All in all, this might be regarded as an upper bound on potential savings, with reference to the $200/dig rule of thumb. The lower bound is zero: Under unfavorable conditions (lossy, heterogeneous soil; a large spectrum of target types with overlapping characteristics; clutter with shapes much like UXO, etc.), GPR use would gain one nothing and would not be applied.

This page left blank intentionally.

6.0 IMPLEMENTATION, DISCUSSION, AND RECOMMENDATIONS

The complexity of the UXO classification problem requires involved processing algorithms to suppress noise and clutter, enhance target response, extract useful features, and improve stability and sensitivity. Although many algorithms have been developed leading up to and during these demonstrations, further developments are necessary for a desirable level of performance in future implementation. While results in terms of some criteria and in some settings are uninspiring (e.g., Figure 4), in others they are strong (Figures 5 and 7). This means that the demonstrated technology may merit use in instances where the kind of savings implied by the latter but not the former figures would apply. That said, we do not in general recommend the application of our system in most circumstances at this time. This is because 1) in the majority of (but not all) circumstances and with the most universal processing criteria (i.e., Figure 4, not Figure 7), the persistently missed detections limit performance stubbornly in the upper portions of the ROC curves; and 2) the newer, much handier, faster, and cheaper GPR that has been developed will likely address the main performance limitations of the system demonstrated. While one cannot always delay application in anticipation of the next generation of improvement, in this instance we feel that the deficiencies in the old system and the capabilities of the emerging system warrant waiting.

Specific and general recommendations appear in this project's final technical progress report. Summarized here, specific recommendations are to:

- *Develop effective algorithms to suppress surface and subsurface clutter*. Techniques are needed to move beyond current systems for suppressing effects of broad, common geophysical structures, such as layers or ground surface. Patterned anomalies such as burrows, trenches, and soil lenses must be dealt with, as well as random signal interactions from clustered targets.
- *Automate data processing and feature extraction procedures*. This can be done. See results of the pilot project in the appendices of this project's final technical progress report.
- *Optimize and automate classification rules*. Broaden classification rules to cover additional cases, beyond canonical shapes and simple clutter type recognition; implement adaptive algorithms to adjust parameter weights, depending on their reliability or importance in conditions at hand, e.g., respond to ambiguous ETO around clustered targets, when resonance is still clear.
- *Develop smaller, lighter, faster antennas to achieve greater ground coverage in a target's locale, e.g., 2-D grids instead of a few lines.* This development is in fact well underway; see the appendices of this project's final technical progress report. Horizontal grids of measurement over easily designated templates would allow (pseudo) 3-D as opposed to the current 2-D views, resolving many ambiguities, as long as measures are undertaken concomitantly.
- *Develop processing for 3-D data obtained from grids.* This could be optimized to be as fast or faster than the current system and would avoid many of the cumbersome and unreliable maneuvers in the current system that result from views along scan lines only.

For identification of general future directions, note that two relatively robust features of the radar records in the face of multitarget scenes are resonance and target position/depth estimation. These suggest a route for exploiting GPR to help address the difficult multitarget (highly contaminated site) problem, as pursued in a current Strategic Environmental Research and Development Program (SERDP) project [4], under circumstances in which EMI is challenged but in which it could excel if cued by the GPR results. Overall, the results of these demonstrations contributed to the case for multisensor surveying, including GPR. The most immediate motivation for this is evident when one considers that the greatest failure in the GPR classifications constituted missed UXOs. This might be avoided by inclusion of Mag or EMI data, both for inference of magnetic dipole type behavior (typical of UXOs) and for estimation of target position, including depth. Many future improvements can be achieved with cooperative processing of GPR and EMI/Mag data, e.g., [18]. This is best done at the "feature level," as cooperative or collaborative processing, as distinct from complete joint inversion. The former has much more relaxed requirements in terms of coregistration of data and algorithmic complexity and potential pathology.

Ideally, one would like to be able to discriminate TRUE UXO even from elongated fragments with lengths comparable to some UXO. Extracting more information on target geometry with GPR would be substantially enhanced by the capability to determine the 3-D scattering pattern, for separating an elongated, plate-like fragment from a cylinder-like UXO. The developing GPR systems mentioned above should be capable of this and might also be used in bi-static mode (separate transmitter and receiver locations) to maximize scattering information.

Particular general directions for optimizing GPR implementation, with or without EMI/Mag collaboration, include:

- *Smart site selection.* This pertains both to the soil and clutter characteristics of the site and also to the nature of the UXO contamination. In sites with limited ordnance diversity and favorable (dry, relatively homogeneous) soil characteristics, classification advances might be achieved comparable to the best shown above.
- *Smart data acceptance/ rejection for individual targets.* The best role for GPR may sometimes not be to supplement Mag/EMI when they are weak but rather simply to pitch in where the GPR proves strong, i.e., when its parameters are clearly identified and confidence in the processing is high. This would not help cases in which GPR was discarded but could achieve considerable savings where it was applicable.
- *Smart interpretative precedence (who helps whom, case by case).* Under some circumstances GPR can produce superior estimates of the number of targets and of target locations and depths [4]. This could then support EMI processing to address other things that, under the particular circumstances at hand, GPR could not do well. GPR typically sees right through shallow, dispersed metallic clutter that blinds EMI to a deeper target. Conversely, under other circumstances (e.g., lossy soil), Mag data might provide superior estimations of target depth/location, which would allow GPR to zero in on the correct positions and perform discrimination at a level that Mag/EMI cannot. In the demonstrations reported here, GPR processing occasionally missed targets by

concentrating on stronger, shallower clutter signals when other technologies could have cued it to focus on appropriately greater depths (BP demonstration).

This page left blank intentionally.

7.0 REFERENCES AND PUBLICATIONS

Publications supported wholly or in part by this ESTCP project are printed in bold blue.

1. *Navy Tri-Service Environmental Quality Research Development, Test and Evaluation Strategic Plan*, October 1994, p. Cleanup-21.

2. U.S. Army Environmental Center. *FY02 Army Environmental Requirements and Technology Assessments (AERTA).* SFIM-AEC-PC-CR-2002040, Final Report, October 2002.

3. Defense Science Board. *Task Force Report on Unexploded Ordnance (UXO) Clearance, Active Range UXO Clearance, and Explosive Ordnance Disposal (EOD) Programs*. Task Force Report to the Office of the Under Secretary of Defense (Acquisition and Technology), April 1998.

4. K. O'Neill, *UXO Discrimination in Cases with Overlapping Signatures*, SERDP Project UX-1282, First Year Report, Mar 2003; Second Year Report, Mar 2004; Third Year Report, Mar 2005.

5. Chi-Chih Chen and L. Peters Jr., "Buried unexploded ordnance identification via complex natural resonances," IEEE Trans. Ant. & Propagat., vol. AP-42, pp. 1645-1654, Nov. 1997.

6. Chi-Chih Chen, " A new ground penetrating radar antenna design—the horn-fed bowtie (HFB)", Antenna Measurement Techniques Association (AMTA) Symposium, October 1997.

7. **K. O'Neill, *Data Processing Results for UXO Classification Using UWB Full-Polarization GPR System,* Mar 2001, ESTCP report. See also OSU/ESL Technical Report 737990-2, M. Higgins and C.-C. Chen: *Dual Broadband Fully Polarized Radar Discrimination of UXO's; Preliminary Data Processing Results for Phase I Tyndall UXO Characterization GPR Measurement,* July 2000.**

8. **Chi-Chih Chen, M. Higgins, K. O'Neill and R. Detsch, "Tyndall AFB measurement results of UXO characterization using full-polarimetric ultra-wide bandwidth (UWB) GPR," UXO Forum, Anaheim, May 2000.**

9. **K. O'Neill, *GPR Classification Results for the Blossom Point Site*, Mar 2002, ESTCP Demonstration Report. See also M.B. Higgins and C.-C. Chen, *GPR UXO Classification Results of The Blossom Point Site*, OSU/ESL Technical Report 737990-6, May 2001.**

10. **K. O'Neill, *GPR UXO Classification Results for Jefferson Proving Ground V*, June 2002, ESTCP Demonstration Report.**

11. **K. O'Neill, *Fort Ord Site UXO Classification Demonstration Using Fully Polarimetric GPR*, July 2002, ESTCP Demonstration Report. See also C.-C. Chen, *Fort Ord Site UXO Classification Demonstration Using Fully Polarimetric GPR*, OSU/ESL Technical Report 737990-9, August 2002.**

12. Chi-Chih Chen, M.B. Higgins, K. O'Neill and R. Detsch, "UWB fully-polarimetric GPR classification of subsurface unexploded ordnance," IEEE Trans. Geosci. & Remote Sensing, Vol. 39, No. 6, pp. 1221-1230, June 2001.

13. H.H. Nelson, J.R. McDonald, and R. Robertson, *Design and Construction of the NRL Baseline Ordnance Classification Test Site at Blossom Point,* Naval Research Laboratory Report NRL/MR/6110—00-8437, March 20, 2000.

14. *ESTCP, Electromagnetic Induction and Magnetic Sensor Fusion for Enhanced UXO Target Classification*, ESTCP Cost and Performance Report, Project UX-9812. See www.estcp.org.

15. *Matched Filter Processor for Detection and Discrimination of Unexploded Ordnance*, ESTCP Cost and Performance Report, Project UX-9918. See www.estcp.org.

16. L. R. Pasion, S.D. Billiings, D.W. Oldenburg, "Joint and cooperative inversion of magnetics and electromagnetic data for the characterization of UXO discrimination problems." Proc. SAGEEP, San Antonio, Texas, U.S.A., Feb 6-10, 2003.

17. B.A. Kramer, M. Lee, Chi-Chih Chen, and J.L. Volakis, "Design and performance of an ultra wideband ceramic-loaded slot spiral," submitted to IEEE Trans. Ant. & Propagat.

18. K. Sun, K. O'Neill, Chi-Chih Chen, H. S. Youn, F. Shubitidze, I. Shamatava, and K. D. Paulsen (2005). Highly contaminated UXO sites: Combination of GPR and EMI for discrimination of clustered scatterers, Symp. Applic. Geophys. to Eng. & Envir. Probl. (SAGEEP) 2005, 3- 7 April, Atlanta.

19. M.D.A. Rahman and K.-B. Yu, "Total least squares approach for frequency estimation using linear prediction," IEEE Transaction on Acoust. Speech Signal Processing, vol. ASSP-35, pp. 1440–1454, Oct. 1987.

20. **K.-H. Lee, N. Venkatarayalu, Chi-Chih Chen, F. Teixeria and R. Lee, *Application of Fully Polarimetric GPR for Buried UXO Classification,* The Ohio State University ElectroScience Laboratory Technical Report 741119-Final, Dec. 2001.**

Additional publications, supported wholly or in part by this ESTCP project:

K.R. Rao, Chi-Chih Chen, R. Lee, and K. O'Neill, "A comparison of broad-bandwidth radar scattering characteristics of buried UXO and non-UXO objects," UXO Forum, Anaheim, May 2-4, 2000.

Chi-Chih Chen, M. Higgins, K. O'Neill and R. Detsch, "UWB full-polarimetric horn-fed bow-tie (HFB) GPR antenna for buried unexploded ordnance (UXO) discrimination," Int'l Geosci. & Remote Sensing Symp (IGARSS) 2000, Honolulu, July 2000, Vol 4, 1430-1432.

M.B. Higgins, Chi-Chih Chen, and K. O'Neill, "Improvement of UXO classification based on fully polarimetric GPR data," Proc. UXO Forum, New Orleans, April 10-12, 2001.

Chi-Chih Chen, M. Higgins, and K. O'Neill, "Improved subsurface UXO discrimination with full-polarimetric, ultra-wideband, ground based radar, using space and frequency

dependent signal features," Workshop on Remote Sensing by Low-frequency Radars, 20-21 September 2001, Naples, Italy.

Chi-Chih Chen, and K. O'Neill, "Performance limitations of the current UWB fully polarimetric GPR in UXO classification," Proc. 9th Int'l Ground Penetrating Radar Conf, Santa Barbara, California, April 29 - May 2, 2002.

Chi-Chih Chen and K. O'Neill, "UWB fully polarimetric GPR database from Tyndall, Blossom Point, Jefferson Proving Ground, and Fort Ord UXO Sites," 9th Int'l Ground Penetrating Radar Conf, Santa Barbara, California, April 29 - May 2, 2002.

Chi-Chih Chen, M. B. Higgins, and K. O'Neill, "Advanced classification of buried UXO using a broadband, fully polarimetric ground penetrating radar," Proc. IGARSS'02, Vol III, 1569-71, Toronto, June 24-28, 2002.

This page left blank intentionally.

APPENDIX A

POINTS OF CONTACT

Point of Contact Name	Organization Name Address	Phone/Fax/email	Role in Project
Dr. Jeffrey Marqusee	ESTCP 901 North Stuart Street Suite 303 Arlington, VA 22203	703-696-2120 703-696-2114 Jeffrey.Marqusee@osd.mil	ESTCP Director
Dr. Anne Andrews	ESTCP 901 North Stuart Street Suite 303 Arlington, VA 22203	703-696-3826 703-696-2114 Anne.Andrews@osd.mil	ESTCP UXO Program Manager
Dr. Kevin O'Neill	ERDC-CRREL 72 Lyme Road Hanover, NH 03755	603-646-4312 603-646-4640 Kevin.O'Neill@erdc.usace.army.mil	Principal Investigator
Dr. Chi-Chih Chen	OSU-ESL 1320 Kinnear Road Columbus, OH 45212	614-292-3403 614-292-7297 Chen.118@osu.edu	Co-Principal Investigator

APPENDIX B

THE GPR PROCESSING SYSTEM

1.1 SIGNAL FEATURE EXTRACTION

1.1.1 Electromagnetic Complex Natural Resonance Feature Extraction [4]

When a UXO is illuminated with broadband electromagnetic fields, the incident fields generate currents on the conducting surface. These currents flow along the UXO's curved surface and generate secondary radiation that is picked up by the radar receiver. The currents flowing circumferentially around the object generate significant radiation only when the circumferential length is comparable to one wavelength in the surrounding medium, or greater, as in the case of a small loop antenna. When the currents flowing axially along the UXO reach the ends, strong diffraction occurs, releasing some energy into the medium while the rest flows back towards the other end. In colloquial language, the induced currents "bounce" back and forth between the ends, with losses radiating into the environment during each trip and reversal. Like the currents flowing circumferentially around the object, those oscillating between the ends exhibit preferential frequencies, depending on the properties of the surrounding medium. Frequencies corresponding to wavelengths containing integral numbers of target surface length will resonate. Typically, the strongest resonant peak is that of the lowest mode, for which the wavelength is approximately twice the target (surface) length. Therefore, the ETL is defined as half the wavelength corresponding to the lowest resonant mode. In practice in the field, the resonant pole is calculated directly from the waveform in the late-time (resonant) region using the modified Prony method [19]. Accurate resonant frequencies can usually be obtained using this method when the magnitude of signal/(noise + clutter) is higher than 10 dB. The target length can be estimated from the resonant frequency and the dielectric properties of the soil measured at each site with a probe.

1.1.2 Late-Time Polarization Feature Extraction [12]

The dominant scattered field from a typical UXO with elongated body is polarized parallel to the UXO axis, as projected onto the antenna (or ground) plane. If the incident electric field is polarized in another direction, only the vector component that is parallel to the UXO axis will generate strong scattering, particularly as the signal fades, and only that component will excite strong resonance (lowest mode).

To obtain late-time resonance information, the measured frequency-domain data werefirst transformed into the time-domain. A late-time region was then selected. Two eigenvalues, $8_{//}$ and 8_{ζ}, were then obtained from this scattering matrix, where $8_{//}$ and 8_{ζ} correspond to the parallel and transverse components of reradiated resonant field intensity, in target coordinates. For a UXO-like target, these correspond to the field components parallel and transverse to the target axis, as projected onto the plane of the antenna (ground surface). The ELF was defined as:

$$\text{ELF} \equiv \text{average}\left\{\left|\frac{\lambda_{//}(t)-\lambda_{\perp}(t)}{\lambda_{//}(t)+\lambda_{\perp}(t)}\right|\right\} \quad t \in \text{late-time region.}$$

In later generations of the processing, the scattering matrix was formed using the signal magnitude readily available in the coefficients of the Prony method during the extraction of resonant features [19].

Solving for the eigenvalues of the scattering matrix also provides eigenvectors, corresponding to the parallel and transverse vectors of the UXO response, in antenna coordinates. The orientation of the dominant eigenvector provides the ETO. As an additional measure of whether or not the target showed a dominant direction of response, as an elongated UXO should, the DEN of responses was determined. The DEN was calculated as the sum of response magnitudes for polarizations $\pm$ 20° on either side of the dominant direction (ETO), divided by the total (integrated) magnitude of response over all directions. Basically, it is a measure of how tightly clustered about the ETO the responses are.

1.1.3 Depth Information Extraction

The target depth was also estimated from the time delay of the earliest reflection, i.e., of the peak of the various hyperbolic arcs shown above. Depending on the UXO orientation, multiple echoes may be received from different parts of the UXO. In such cases, the shallowest point was chosen to correspond to the "depth." Both length and depth estimation must be done in conjunction with a proper estimation of soil electrical properties, which were measured using an OSU soil probe. The good quality of the depth estimations shown in the individual demonstration reports, when targets produced unequivocal reflections, attests to the accuracy of the probe data. Dielectric constant measurement was usually done at the beginning of each day of survey, requiring only about half an hour, and could be done less frequently when environmental conditions do not change.

1.1.4 Parameter Extraction Processing Summary

The data processing and feature extraction procedure adopted is summarized in the following block diagram, explained step by step below.

Step 1: After the software plots signal magnitudes in time versus antenna position and frequency versus position on the display, the operator selects a modified time range or frequency band, if desired.

Step 2: The truncated step-frequency data are transformed into time domain using inverse fast Fourier transform (IFFT) for each position X_n. Next, the operator inspects the time versus position GPR plots of S_{11}, S_{21}, and S_{22} channels to pick the channel that shows the best SCR, i.e., clearest target responses. This channel will be used for determining the spatial filter in the next step. If none of the channels show recognizable target responses, go back to Step 1 and try a different time range/band. Typically, a three-band approach—low band, middle band and high band—should be sufficient. If the target responses are still invisible, then declare no target. If the SCR is good and the target responses are clear, there is no need to

change the frequency range. Otherwise, enter the desired start and stop frequencies. If the target responses contain frequency content that is either very high or very low, adjust the frequency range to enhance the SCR.

Step 3: Select more than five points along a prominent hyperbolic response pattern (broken or not broken) in the space-time plot, for adaptive spatial smoothing. The GPR data of all three channels is replotted after the spatial smoothing. The points do not need to be selected in any order, but the waveform corresponding to the position of the first point will be used as an example waveform for determining the duration of the late-time region in the next step.

Step 4: Select the start- and stop-time positions from the example waveform to define the late-time region for obtaining the late-time spectrum by transforming the waveform in the late-time region into frequency domain using fast Fourier transformation. The difference between the start- and stop-time positions also determines the length of the late-time region that will be used for feature extraction.

Step 5: A late-time spectrum obtained from the previous step is plotted. The operator now selects the center frequency (frequency peak) and the half-width of a bandpass filter.

Step 6: Apply the bandpass filter determined from the previous step to the background subtracted data (all channels) as used in Step 1.

Step 7: Transform the filtered data into time domain. Now the resonant signal should appear enhanced.

Step 8: Repeat Step 2 to apply the spatial smoothing to reduce interference from other scattering sources.

Step 9: This step selects the target region to be focused on for feature extraction and investigation. This is done by selecting two diagonal points of a rectangular region that boxes most of the target-related responses.

Step 10: This step determines the onset of the late-time region for every position. This is done by first manually selecting a few points on the strongest signal arc in the replotted time versus position data. The software then automatically traces out maximum magnitude pixels along the arc. Each such pixel becomes the onset time of the late-time region for a given antenna position associated with that pixel. Recall that the duration of each late-time region is the same as was determined in Step 3. Note that the late-time regions for all three channels will be the same.

Step 11: For each antenna position within the target region selected in Step 8, Prony's method is applied to the response in the late-time region to extract the resonant frequency, damping factor, and initial resonant amplitude. The resonant amplitude is given by the magnitude of the Prony's coefficient associated with each resonant mode.

Step 12: The resonant amplitudes obtained from S_{11}, S_{21}, and S_{22} channels are then used to form a scattering matrix, from which the eigenvalues and eigenvectors are obtained. Polarization signatures are then calculated from the eigenvalues and eigenvectors, as discussed above.

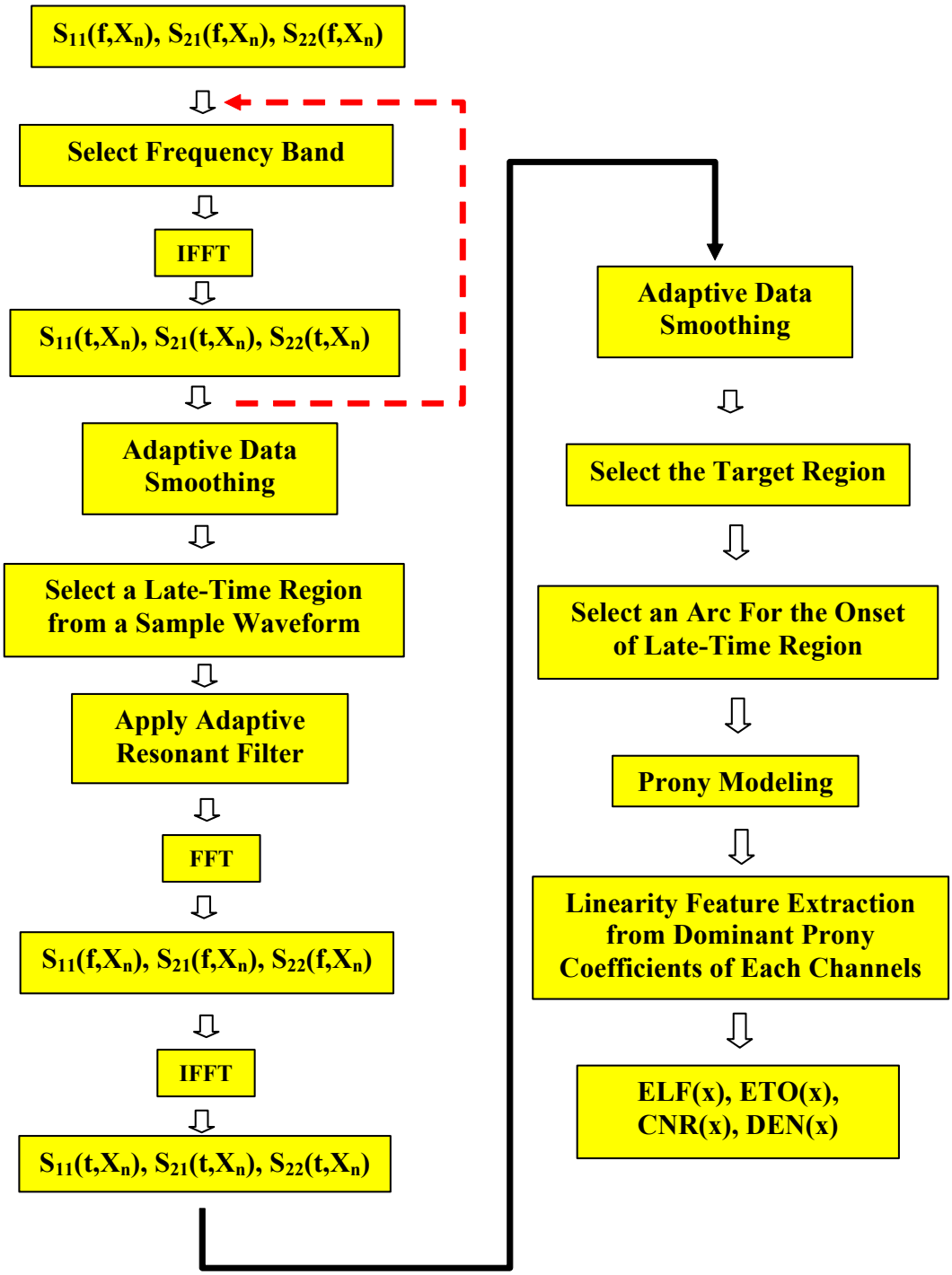

Full Polarimetric, UWB GPR Data Processing and Feature Extraction Procedures for UXO Classification.

1.2 UXO CLASSIFICATION RULES AND PROCESSING

A set of classification rules was developed to discriminate UXO-like items (usually L/D ratio greater than three) from other metallic objects. These rules are organized in a classification tree, illustrated in the graphic below. This classification tree was finalized for the JPG-V and Fort Ord tests. The rules were based predominantly on late-time polarization features (ELF and ETO) as a function of antenna position and scan orientation. Several rules involve qualitative spatial pattern recognition. All characteristics in the qualitative descriptions that are sought "by eye" can be shown to have a solid physical basis, based on rigorous numerical model simulations [20]. Further, recognition of the essential features has been automated during work following this project.

The whole UXO classification procedure starts with inspection of the spatial distribution of ELF values. This distribution has five categories (A-E), as illustrated in the graphic at the top layer of the tree. Since data have been collected from different passes, it is easiest to start with the pass that has strongest target responses or has the best SCR. Then, other passes can be used as a secondary confirmation at lower layers of the tree. Each rule is discussed briefly in the list below. The classification criteria were found to be very effective if all GPR scans passed through the target, i.e., directly over its position. Classification error occurs when some or none of the scans passes through the target position. Alleviation of this problem is discussed in the concluding section of this report.

Rule A: If the target has a high SCR and the ELF is low over one antenna width, this indicates that the target is not UXO-like due to low linearity.

Rule B: If the ELF values are high (> 0.6) near the target region, the object could be a UXO-like object, a vertical plate or a vertically oriented bent metal object such as a horseshoe. Proceed to Rule F.

Rule C: If two elevated ELF regions next to the target center are observed (double peaks), the object could be a vertical UXO or shallow clutter that couples to the arms of antenna #1 strongly. Proceed to Rule G.

Rule D: If there is a region of high ELF values and it is offset to one side of target response (single peak), it is probably a moderately inclined UXO-like object or a horizontal UXO-like object with a position offset along the scan direction. In this case, the ETO near the high ELF region should remain unchanged regardless of the scan direction.

Rule E: If the response is weak and the ELF values vary drastically between 0 and 1 in a sort of random way, this is either an empty site or a deep target with poor SCR.

Rule F: In this rule, the time versus position GPR data collected from a pass transverse to the ETO is examined. The dashed line in the block diagram indicates the scan direction. In this pass, a horizontal UXO-like object should have strong S_{22} response but very weak S_{11} response at all positions. If a strong scattering magnitude is observed in the S_{11} data at offset positions such that the scattering pattern appears as broken hyperbolic arcs, the object is not classed as UXO-like. It could be a thick vertical plate, vertical horseshoe, vertical bent wire, etc. The high ELF center observed in Rule B is caused by scattering from the top edge.

Stronger S_{11} response at offset positions in the transverse pass is caused by scattering from the rest of the body when observed from its side. If the S_{11} scattering pattern does not show broken arcs, proceed to Rule H.

Rule G: In this rule, the time versus position GPR data from S_{11} and S_{22} channels are examined simultaneously. A vertical UXO-like object would have a weak scattering magnitude when measured directly above due to relatively small cross-sectional area compared to the wavelength. The scattering magnitude increases as the incident angle moves away from its axis. This would produce broken hyperbolic arcs in the S_{11} data. The magnitude of the S_{22} data should remain weak away from the target center because the electric field polarization is transverse to the UXO axis. Therefore, if a strong scattering magnitude is observed near the target center with complete arcs in both S_{11} and S_{22} data regardless of the scan direction, this indicates a non-UXO item: The high ELF region observed in Rule C is caused by coupling to the arms of antenna #1. In this case, the ETO would also be the same as the scan direction in all passes.

Rule H: In this rule, the ETOs obtained from all passes are examined simultaneously. The dashed lines indicate the scan directions. A horizontal UXO-like object should register a similar ETO regardless of scan direction. When the ETOs are significantly different (>20 degrees) from pass to pass, the object is not likely to be a horizontal UXO.

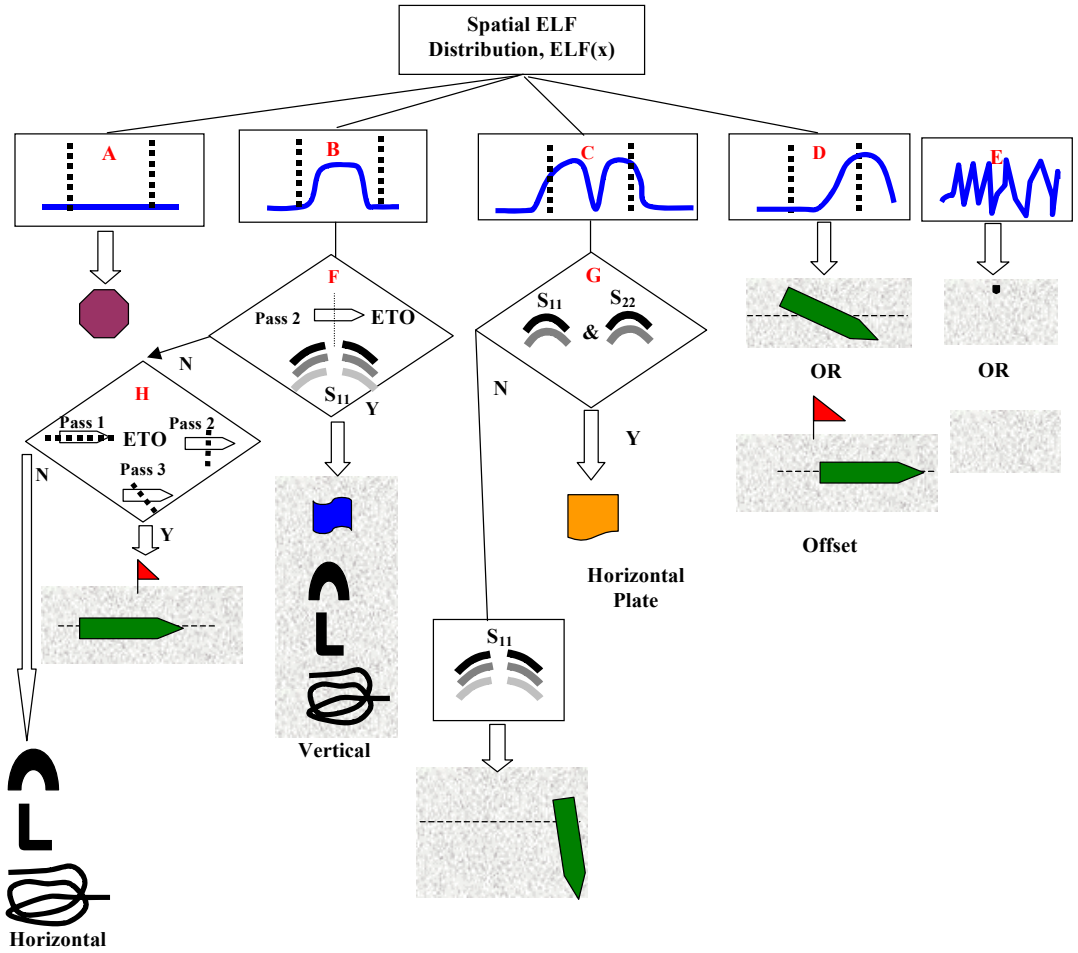

Target Classification Rule Structure Based on GPR Signatures.

ESTCP Program Office

901 North Stuart Street
Suite 303
Arlington, Virginia 22203

(703) 696-2117 (Phone)
(703) 696-2114 (Fax)

e-mail: estcp@estcp.org
www.estcp.org